AIMS Mathematics, 8(7): 16926–16960.
DOI: 10.3934/math.2023865
Received: 02 March 2023
Revised: 18 April 2023
Accepted: 24 April 2023
Published: 15 May 2023

http://www.aimspress.com/journal/Math

Research article

Optimal control analysis of Monkeypox disease with the impact of environmental transmission

Ahmed Alshehri[1] **and Saif Ullah**[2,*]

[1] Department of Mathematics, Faculty of Sciences, King Abdulaziz University, Jeddah, 21589, Saudi Arabia

[2] Department of Mathematics, University of Peshawar, Khyber Pakhtunkhwa, Pakistan

* **Correspondence:** Email: saifullah.maths@uop.edu.pk.

Abstract: Monkeypox is an emerging zoonotic viral disease resembling that of smallpox, although it is clinically less severe. Following the COVID-19 outbreak, monkeypox is an additional global health concern. The present study aims to formulate a novel mathematical model to examine various epidemiological aspects and to suggest optimized control strategies for the ongoing outbreak. The environmental viral concentration plays an important role in disease incidence. Therefore, in this study, we consider the impact of the environmental viral concentration on disease dynamics and control. The model is first constructed with constant control measures.The basic mathematical properties including equilibria, stability, and reproduction number of the monkeypox model are presented. Furthermore, using the nonlinear least square method, we estimate the model parameters from the actual cases reported in the USA during a recent outbreak in 2022. Normalized sensitivity analysis is performed to develop the optimal control problem. Based on the sensitivity indices of the model parameters, the model is reformulated by introducing six control variables. Based on theoretical and simulation results, we conclude that considering all suggested control measures simultaneously is the effective and optimal strategy to curtail the infection. We believe that the outcomes of this study will be helpful in understanding the dynamics and prevention of upcoming monkeypox outbreaks.

Keywords: Monkeypox outbreak 2022; environmental transmissions; parameter estimation; Pontryagin's maximum principle
Mathematics Subject Classification: 37N25, 34D23, 34H05

1. Introduction

Classified under the orthopoxvirus genus of the Poxviridae family, the monkeypox virus (MPXV) is responsible for the onset of the viral disease monkeypox (MPX) [1]. The first human case of

MPX was reported in 1958 and was distinguished them from smallpox at the start of 1970s. Every continent, with the exception of Antarctica, has recorded more than 15,000 infected cases of MPX since May 2022 [2]. The smallpox-like MPXV causes MPX, a contagious zoonotic disease [3, 4]. Transmission through animal-to-human, human-to-human, and environmental factors (inter- or intra-human) are the three considerable and possible routes that MPXV might spread. Animals (particularly rodents) and humans commonly come into direct contact and spread infections. Although, the infection cases have been observed in various non-endemic countries in the world, it is typically found in Africa. The typical symptoms of MPX include fever, chills, and a rash that develops after a few days. Animals of many different species can contract the MPXV. The incubation period of monkeypox in humans is commonly from 6 to 13 days, but can range from 5 to 21 days [1]. In order to identify the specific reservoir(s) and to understand how virus flow is regulated in nature, more research is required to understand the MPXV. Eating raw meat and other animal products that have been in contact with infected animals may pose a risk [5]. In non-endemic countries where cases have been discovered, additional public health measures are adopted, including thorough contact tracing and case discovery, laboratory analysis, diagnostic procedure, and isolation with supportive therapy. When possible, genomic sequencing has been employed to pinpoint the viral clade(s) causing this outbreak of MPX. Despite the fact that there are currently no specific treatments for MPX infection, outbreaks can be managed. While smallpox has been eradicated worldwide, the vaccine ST-246 and antiviral medications like tecovirimat, Cidofovir, and Brincidofovir designed for use in smallpox patients may help in the fight against MPX. However, these medications are not yet available commercially [6]. The Centers for Disease Control and Prevention (CDC) recommendation was developed using the most up-to-date data on the advantages and risks of smallpox immunization and treatments for MPX and other orthopoxvirus infections. The absence of a proper understanding of the MPXV disease's transmission dynamics and associated factors creates an environment that is conducive to the disease's incidence in both endemic and non-endemic regions.

Epidemic models have been used by numerous researchers to investigate the prevalence of infection outbreaks in different regions, and they have shown to be useful and reliable tools [7, 8]. Many models have been created and investigated using a variety of approaches in order to better illustrate the dynamics of the disease's spread and control [9, 10]. Researchers Somma [11], Lasisi [12], Usman, and Adamu [13], and Emeka [14] have formulated mathematical models of MPX with two host populations. To eradicate the spread of MPX, Somma [11] studied the impact of public awareness and quarantine strategy, whereas Lasisi [12] implemented an exposed population group for both human and animal populations, in addition to a vaccine class for migrants. To better understand the spread of MPXV infection Usman and Adamu [13] looked into the effectiveness of combined vaccine and therapy measures. On the other hand, Emeka et al. [14] developed a deterministic model where they examined how an incomplete vaccination might affect the dynamics of infection. For the purpose of analyzing the dynamics of the MPX in the human population, the authors of [15] formulated a deterministic mathematical model. These results imply that separating infected individuals from the broader community lessens the spread of disease. In [16], a novel approach based on fractional calculus and fractal theory was used to investigate human-to-animal transmission. Madubueze et al. [17] was the first to demonstrate how the dynamics of MPX are affected by a polluted environment (i.e., surfaces and materials that have been exposed to MPX by environmental viral shedding).

The optimal control approach is an effective tool used to find the best and optimum control strategy

for a system to achieve a desired objective [18, 19]. In optimal control theory, a system is typically converted to a set of differential equations describing the evolution of the system over time, and the control strategy is represented as a function that maps the current state of the system to a control input. The goal of optimal control theory is to find the control strategy that either minimizes or maximizes an objective function, subject to constraints on the system and the control input [20]. There are various approaches to solving optimal control problems, including analytical methods and numerical optimization techniques. Some common numerical methods used to solve the optimized problem include Pontryagin's maximum principle, dynamic programming, and model predictive control [21]. Application of optimal control theory to set the optimal strategies for an infectious disease eradication including MPX can be found in [22, 23].

Despite the aforementioned discussion, MPX still persists in the population. We analyze the dynamics of MPX with the environment transmission routes in the presence of optimized preventive strategies. Moreover, the influence of some crucial factors on disease prevalence is identified and health officials are advised. This study is structured as follows: Construction of the epidemic model for the MPX dynamics and the estimation procedure are presented in section 2. The basic analysis of the proposed model is covered in section 3. Section 4, accomplishes the normalized sensitivity analysis of the parameters of the proposed model versus $\mathcal{R}_0$. In section 5, the construction of the optimal control system along with the solution and existence of the problem is presented. Simulation with comprehensive discussion are provided in section 6. The concluding remarks with future directions are mentioned in section 7.

2. Mathematical formulation of the MPX dynamics

This section presents the construction of the mathematical model for the transmission dynamics of MPX using a system of nonlinear differential equations. Two populations i.e. humans and animals (those capable to transmit the infection) are considered to formulate the model. The MPX model for the human population consists of four compartments, S_h, I_h, Q_h, and R_h; the animal population is classified in two sub-classes, the susceptible S_r and the infectious class I_r. The viral contamination due to the environment is denoted by E_n. The cumulative population in both human and animal cases are shown as follows:

$$N_h(t) = S_h(t) + I_h(t) + Q_h(t) + R_h(t),$$
$$N_r(t) = S_r(t) + I_r(t).$$

2.1. Mathematical model for human sub-population

The susceptible human population recruits through the rate λ_h and through the progression of the isolated population to susceptible at rate τ_1. This class is decreased by the force of infection $\lambda_h = \frac{\beta_1 I_r}{N_r} + \frac{\beta_2 I_h}{N_h} + \frac{\zeta E_n}{k+E_n}$, where β_1, β_2, and ζ are the human to human, animals to humans, and environmental transmission rates, respectively. Moreover, the human natural mortality rate is denoted as μ_h.

The class of infected humans is increased due to the progression of susceptible individuals at the rate λ_h after getting the infection. The class of infected individuals is also reduced by the rates, μ_h (the natural death rate), ϕ (the progression of I_h to Q_h), δ (the MPX-induced mortality rate), and γ the infected humans recovery rate.

Progression of infected individuals I_h to isolated individuals at the rate ϕ form the class Q_h, where τ_1 represents the transfer of the isolated/quarantined individuals to susceptible people and τ_2 is the recovery rate.

The infected and quarantine individuals join the recovered class after recovery from infection. This class is also decreased by the same natural death rate. Thus, the sub-model for the only human population is organized in the following system:

$$\begin{aligned}
\frac{dS_h}{dt} &= \Lambda_h - (\frac{\beta_1 I_r}{N_r} + \frac{\beta_2 I_h}{N_h} + \frac{\zeta E_n}{k+E_n})S_h + \tau_1 Q_h - \mu_h S_h,\\
\frac{dI_h}{dt} &= (\frac{\beta_1 I_r}{N_r} + \frac{\beta_2 I_h}{N_h} + \frac{\zeta E_n}{k+E_n})S_h - (\phi + \gamma + \mu_h + \delta)I_h,\\
\frac{dQ_h}{dt} &= \phi I_h - (\tau_1 + \tau_2 + \mu_h)Q_h,\\
\frac{dR_h}{dt} &= \gamma I_h + \tau_2 Q_h - \mu_h R_h.
\end{aligned} \tag{2.1}$$

2.2. Mathematical model for animals sub-population

The class of susceptible animals is recruited with a recruitment rate Λ_r. This class is decreased by λ_r due to the interaction of susceptible animals with infected ones. This is further reduced at the rate μ_r due to natural death. The infected animals are increased by joining the susceptible animals at the infection force λ_r and decreased by the natural mortality rates μ_r. Thus, the sub-model describing the dynamics of only animals is described as follows:

$$\begin{aligned}
\frac{dS_r}{dt} &= \Lambda_r - \frac{\beta_3 I_r}{N_r} S_r - \mu_r S_r,\\
\frac{dI_r}{dt} &= \frac{\beta_3 I_r}{N_r} S_r - \mu_r I_r.
\end{aligned} \tag{2.2}$$

2.3. Environment concentration of MPXV

When the infected individuals (humans or animals) shed infection to the environment, it affects the infection force term λ_h. Therefore, the environmental viral concentration has an important role in disease transmission. Regarding the choice of the incidence function, there are a number of choices present in the literature [24, 25]. In this study, we consider the saturated incidence rate for the concentration of the MPX disease within the environment. The following is one way that MPXV might spread indirectly and how long it can live in the environment.

$$\frac{\zeta E_n}{k + E_n}.$$

The concentration of the MPXV in the environment increases when infected individuals and rodents release the pathogen at rates of ρ_1 and ρ_2, respectively, and decreases due to decay with rate ν_n. Thus, the equation below describes the dynamics of the environmental viral concentration.

$$\frac{dE_n}{dt} = \rho_1 I_h + \rho_2 I_r - \nu_n E_n. \tag{2.3}$$

Combining Eqs (2.1) to (2.3), we have the following dynamical system:

$$\begin{aligned}
\frac{dS_h}{dt} &= \Lambda_h - \lambda_h S_h + \tau_1 Q_h - \mu_h S_h,\\
\frac{dI_h}{dt} &= \lambda_h S_h - l_1 I_h,\\
\frac{dQ_h}{dt} &= \phi I_h - l_2 Q_h,\\
\frac{dR_h}{dt} &= \gamma I_h + \tau_2 Q_h - \mu_h R_h,\\
\frac{dS_r}{dt} &= \Lambda_r - \lambda_r S_r - \mu_r S_r,\\
\frac{dI_r}{dt} &= \lambda_r S_r - \mu_r I_r,\\
\frac{dE_n}{dt} &= \rho_1 I_h + \rho_2 I_r - \nu_n E_n,
\end{aligned} \tag{2.4}$$

where

$$\lambda_h = \frac{\beta_1 I_r}{N_r} + \frac{\beta_2 I_h}{N_h} + \frac{\zeta E_n}{k + E_n},\ \lambda_r = \frac{\beta_3 I_r}{N_r},\ l_1 = (\phi + \gamma + \mu_h + \delta),\ and\ l_2 = (\tau_1 + \tau_2 + \mu_h),$$

subject to nonnegative initial conditions (ICs)

$$\begin{aligned}
S_h(0) &= \bar{S}_{h_0} \geq 0,\ I_h(0) = \bar{I}_{h_0} \geq 0,\ Q_h(0) = \bar{Q}_{h_0} \geq 0,\ R_h(0) = \bar{R}_{h_0} \geq 0,\\
S_r(0) &= \bar{S}_{h_0} \geq 0,\ I_r(0) = \bar{I}_{r_0} \geq 0,\ E_n(0) = \bar{E}_{n_0} \geq 0.
\end{aligned} \tag{2.5}$$

The transition among different population groups can be easily understood from Figure 1.

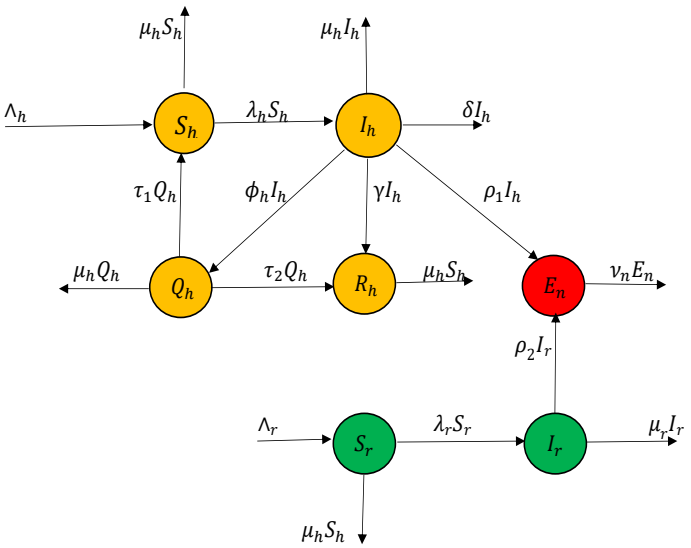

(a)

Figure 1. Flow diagram of model (2.4).

2.4. *Data fitting and parameter estimation*

This section briefly addresses the parameter estimation procedure for the MPX model (2.4) using a nonlinear standard least square approach based on residual minimization. Furthermore, some of the demographic parameters (i.e., Λ_h, μ_h) are estimated from the literature [26]. The values of parameters Λ_r, μ_r and K are taken from [17]. For the rest of the model parameters, the actual reported cases in the recent outbreak in the USA during 2022 are taken into the account to provide a reasonable fitting by the model simulation. The best fit provided by the proposed epidemic model to the real data is depicted in Figure 2. The respective parameters with biological descriptions and numerical values are tabulated in Table 1.

Table 1. Fitted and estimated values of parameters.

Parameter	description	Value in days	Reference
Λ_h	Birth rate of humans	11731.91	[26]
Λ_r	Birth rate of animals	0.2	[17]
μ_h	Humans mortality rate	$\frac{1}{79\times365}$	[26]
μ_r	Animals mortality rate	0.04	[24]
ν_n	Decay rate of monkeypox virus in environment	0.003	[24]
γ	I_h recovery rate	0.1490	Fitted
β_1	Animals to human transmission rate	2.0000×10^{-5}	Fitted
β_2	Human to human transmission rate	0.2084	Fitted
ζ	Environmental transmission rate	3.0791×10^{-7}	Fitted
β_3	Rodents to rodents transmission rate	0.0694	Fitted
K	Environmental viral concentration	500	[17]
ρ_1	Shedding rate due I_h in the environment	0.04	Fitted
ρ_2	Shedding rate due I_r in the environment	0.02	Fitted
δ	Monkeypox induced death rate	0.1478	Fitted
τ_1	Progression rate of quarantined individuals to S_h	0.4977	Fitted
τ_2	Recovery rate of Q_h class	3.5430×10^{-4}	Fitted
ϕ	Progression rate of I_h to Q_h	0.1623	Fitted

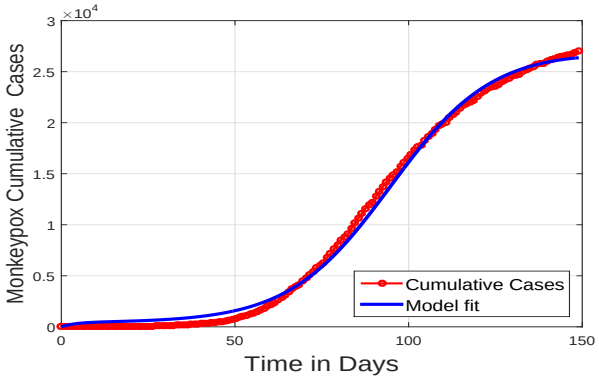

Figure 2. The blue solid curve show the simulated curve of infected population while the circles red curve illustrate the reported infected cases.

3. Basic analysis of the model

3.1. Positivity and invariant region

Theorem 3.1. *The solution* $\mathcal{G}(t) = (S_h(t), I_h(t), Q_h(t), R_h(t), S_r(t), I_r(t), E_n(t))$ *with non-negative initial condition of the model (2.4) will be positive for* $t \geq 0$, *also* $lim_{t\to\infty} SupN_h \leq \frac{\Lambda_h}{\mu_h}$, $lim_{t\to\infty} SupN_r = \frac{\Lambda_r}{\mu_r}$ *and* $E_n(t) \leq \frac{1}{\nu_n}\left(\frac{\rho_1\Lambda_r}{\mu_r} + \frac{\rho_2\Lambda_h}{\mu_h}\right)$.

Proof. Let the initial conation of the MPX problem is $\mathcal{G}(0)$, which is non-negative. In order to prove our required result, we consider the first the equation of system (2.4) and proceed as follows:

$$\frac{dS_h}{dt} = \Lambda_h - (\lambda_h + \mu_h)S_h + \tau_1 Q_h \geq \Lambda_h - (\lambda_h + \mu_h)S_h,$$

which can further be written as

$$\frac{d}{dt}\Big(S_h(t)\exp(\mu_h t + \int_0^t \lambda_h(\xi)d\xi)\Big) \geq \Lambda_h\Big(\exp(\mu_h t + \int_0^t \Lambda_h(\xi)d\xi)\Big).$$

By integrating, we have

$$S_h(\tau) \geq S_h(0)\left(\exp\left(-\left(\mu_h\tau + \int_0^\tau \lambda_h(\xi)\,d\xi\right)\right)\right) + \exp\left(-\left(\mu_h\tau + \int_0^\tau \lambda_h(\xi)\,d\xi\right)\right)$$
$$\times \int_0^\tau \lambda_h\left(\exp(\mu_h\psi) + \int_0^\psi \lambda_h(\xi)\,d\xi\right)d\psi > 0.$$

Similarly, for other equations of the MPX model (2.4), we obtain the desired interpretation. To prove the subsequent part of theorem, consider the human and animal populations separately involved in the system (2.4), we have

$$\frac{dN_h}{dt} = \Lambda_h - \delta I_h - \mu_h N_h,$$

$$\frac{dN_h}{dt} \leq \Lambda_h - \mu_h N_h.$$

By simple manipulation, we have

$$N_h(t) \leq N_h(0)\,e^{-\mu_h t} + e^{-\mu_h t}\int_0^t \Lambda_h e^{-\mu_h\xi}d\xi$$

$$\leq N_h(0) \times e^{-\mu_h t} + \frac{\Lambda_h}{\mu_h}\left(1 - e^{-\mu_h t}\right),$$

$$\lim_{t\to\infty} SupN_h(t) \leq \frac{\Lambda_h}{\mu_h}.$$

In a similar way, we can prove that $\lim_{t\to\infty} SupN_r(t) = \frac{\Lambda_r}{\mu_r}$. Since $I_h \leq N_h$ and $I_r \leq N_r$, we have from last equation of model (2.4) that

$$\frac{dE_n}{dt} = \rho_1 I_h + \rho_2 I_r - \nu_n E_n,$$

$$\frac{dE_n}{dt} + \nu_n E_n \leq \left(\frac{\rho_1\Lambda_h}{\mu_h} + \frac{\rho_2\Lambda_r}{\mu_r}\right),$$

which implies that

$$E_n \leq \frac{1}{\nu_n}\left(\frac{\rho_1\Lambda_h}{\mu_h} + \frac{\rho_2\Lambda_r}{\mu_r}\right).$$

Hence, the biological feasible region is given by

$$\Theta = \begin{cases} (S_h, I_h, Q_h, R_h, E_n) \in \mathbb{R}_+^5 : 0 \leq N_h(t) \leq \frac{\Lambda_h}{\mu_h}, \\ (S_r, I_r) \in \mathbb{R}_+^2 : 0 \leq N_r(t) \leq \frac{\Lambda_r}{\mu_r}, \\ E_n \leq \frac{1}{\nu_n}\left(\frac{\rho_1\Lambda_h}{\mu_h} + \frac{\rho_2\Lambda_r}{\mu_r}\right). \end{cases}$$

□

Proposition 3.2. *For non-negative ICs, the region defined above in* Θ *is bounded as well as positively invariant in* $\mathbb{R}_+^5 \times \mathbb{R}_+^2$.

Proof. We know form Theorem 3.1,

$$\begin{array}{l} \frac{dN_h}{dt} \leq \Lambda_h - \mu_h N_h, \\ \textit{and} \\ \frac{dN_r}{dt} \leq \Lambda_r - \mu_r N_r. \end{array} \tag{3.1}$$

After some simplification, we have

$$\begin{array}{l} N_h \leq e^{-\mu_h t} N_h(0) + \frac{\Lambda_h}{\mu_h}\left(1 - e^{-\mu_h t}\right), \\ \textit{and} \\ N_r \leq e^{-\mu_r t} N_r(0) + \frac{\Lambda_r}{\mu_r}\left(1 - e^{-\mu_r t}\right). \end{array} \tag{3.2}$$

Particularly, we have $N_h \leq \frac{\Lambda_h}{\mu_h}$ and $N_r \leq \frac{\Lambda_r}{\mu_r}$. Additionally, from the last equation of system (2.4) we have,

$$E_n \leq \frac{1}{\nu_n}\left(\frac{\rho_1\Lambda_h}{\mu_h} + \frac{\rho_2\Lambda_r}{\mu_r}\right). \tag{3.3}$$

Hence, the set shown by Θ is positively invariant. Furthermore, all solution trajectories will attract in $\mathbb{R}_+^5 \times \mathbb{R}_+^2$. □

3.2. Existence of equilibrium points and $\mathcal{R}_0$

This section presents the evaluation and existence of the model equilibria. The basic reproductive number $\mathcal{R}_0$, one of the essential and threshold parameters in epidemiology, is also evaluated in this part. Model (2.4) possess two equilibrium points: the monkeypox free equilibrium (`MPXFE`), and the monkeypox endemic equilibrium (`MPXEE`). The `MPXFE` point is given by

$$\mathcal{M}^0 = \left(S_h^0, I_h^0, Q_h^0, R_h^0, S_r^0, I_r^0, E_n^0\right) = \left(\frac{\Lambda_h}{\mu_h}, 0, 0, 0, \frac{\Lambda_r}{\mu_r}, 0, 0\right). \tag{3.4}$$

The $\mathcal{R}_0$ is computed via the well-known next-generation technique [27]. The resulting expression of the $\mathcal{R}_0$ is as follows

$$\mathcal{R}_0 = \max\left\{\mathcal{R}_r^0, \mathcal{R}_h^0\right\} = \max\left\{\mathcal{R}_r^0, \mathcal{R}_{h_1}^0 + \mathcal{R}_{h_2}^0\right\} = \max\left\{\frac{\beta_3}{\mu_r}, \frac{\beta_2}{l_1} + \frac{\zeta\Lambda_h\rho_1}{\nu_n k\mu_h l_1}\right\}, \tag{3.5}$$

where

$$\mathcal{R}_r^0 = \frac{\beta_3}{\mu_r}, \quad \mathcal{R}_{h_1}^0 = \frac{\beta_2}{l_1} \quad \mathcal{R}_{h_1}^0 = \frac{\zeta\Lambda_h\rho_1}{\nu_n k\mu_h l_1}.$$

3.2.1. MPX endemic equilibrium point

By simultaneously solving the human, rodent, and environmental classes of the system (2.4) at steady state denoted by $\mathcal{M}_{ee} = (S_{h_{ee}}, I_{h_{ee}}, Q_{h_{ee}}, R_{h_{ee}}, S_{r_{ee}}, I_{r_{ee}}, E_{n_{ee}})$, where

$$\begin{aligned}
S_{h_{ee}} &= \tfrac{l_1 l_2 \Lambda_h}{l_1 l_2(\lambda_{h_{ee}}+\mu_h)-\phi\lambda_{h_{ee}}\tau_1},\\
I_{h_{ee}} &= \tfrac{\lambda_{h_{ee}}}{l_1} S_{h_{ee}},\\
Q_{h_{ee}} &= \tfrac{\phi}{l_2} I_{h_{ee}},\\
R_{h_{ee}} &= \tfrac{\gamma I_{h_{ee}}+\tau_2 Q_{h_{ee}}}{\mu_h},\\
S_{r_{ee}} &= \tfrac{\Lambda_r}{\beta_3},\\
I_{r_{ee}} &= \tfrac{\lambda_{r_{ee}}}{\mu_r} S_{r_{ee}},\\
E_{n_{ee}} &= \tfrac{\rho_1 I_{h_{ee}}+\rho_2 I_{r_{ee}}}{\nu_n}.
\end{aligned} \tag{3.6}$$

Consider force of the infection term as follows

$$\lambda_{h_{ee}} = \frac{\beta_1 I_{r_{ee}}}{N_{r_{ee}}} + \frac{\beta_2 I_{h_{ee}}}{N_{h_{ee}}} + \frac{\zeta E_{n_{ee}}}{k + E_{n_{ee}}}. \tag{3.7}$$

We obtain the following polynomial by using in (3.6) in (3.7)

$$b_0\left(\lambda_{h_{ee}}\right)^3 + b_1(\lambda_{h_{ee}})^2 + b_2\lambda_{h_{ee}} + b_3 = 0, \tag{3.8}$$

where

$$b_3 = -\frac{S_{r_{ee}}\left(\mathcal{R}_r^0-1\right)l_1^2l_2^2}{\beta_3}\left(k\beta_1\beta_2\nu_n + \left(S_{r_{ee}}\left(\mathcal{R}_r^0-1\right)\beta_3 + \zeta\Lambda_r\right)\rho_2\right),$$

$$b_2 = -\left(\mathcal{R}_r^0-1\right)S_{r_{ee}}l_1l_2\left\{\begin{array}{l}\left(\Lambda_h k\nu_n + \rho_2\left(\left(\Lambda_h\left(\beta_1+1\right)+1\right)\left(\mathcal{R}_r^0-1\right)S_{r_{ee}}\right)\right)\left(l_1l_2-\phi\tau_1\right)+\\ \phi\left(k\Lambda_h\beta_1\nu_n + \left(\mathcal{R}_r^0-1\right)S_{r_{ee}}\left(\Lambda_h\rho_2\left(\zeta+\beta_1+1\right)\right)\right)\left(\mu_h+\tau_2\right)+\\ \Lambda_h k\nu_n l_2\beta_1\left(\gamma+\mu_h\right)+\Lambda_h k\nu_n l_1l_2\mu_h R_r^0\left(\mathcal{R}_h^0-1\right)+S_{r_{ee}}l_2\zeta\Lambda_h\rho_2\\ \left(\gamma+\mu_h\right)+\Lambda_h\rho_2 l_1l_2\mu_h\left(\mathcal{R}_r^0-1\right)S_{r_{ee}}\left(\mathcal{R}_{h_1}^0-1\right)\left(1+S_{r_{ee}}\right)+l_2\beta_1\Lambda_h\\ \left(\left(\gamma+\mu_h\right)\rho_2+\Lambda_h\rho_1\right)+\left(\mathcal{R}_r^0-1\right)S_{r_{ee}}l_2\rho_2\Lambda_h\left(\zeta\left(\gamma+\mu_h\right)\right)\end{array}\right\},$$

$$b_1 = -\left\{\begin{array}{l}\left(l_1l_2-\phi\tau_1\right)\left(\left(\mathcal{R}_{h_1}^0-1\right)f_1+\left(\gamma+\mu_h\right)f_2+\phi\left(\mu_h+\tau_2\right)f_3\right)+\left(\mathcal{R}_r^0S_{r_{ee}}\left(\mathcal{R}_{h_1}^0-1\right)l_1l_2^2\Lambda_h\rho_1\right)\\ l_2\left(\gamma+\mu_h\right)S_{r_{ee}}\left(\begin{array}{l}kl_1l_2\Lambda_h\nu_n\left(\mathcal{R}_{h_2}^0-1\right)+\left(\mathcal{R}_r^0-1\right)l_2\Lambda_h\left(\left(\beta_1\rho_1+\zeta+l_1\rho_2\left(R_r^0-1\right)\right)S_{h_{fe}}\right)\\ -l_1\left(\mathcal{R}_r^0-1\right)\left(S_{r_{ee}}\rho_2+kl_2\Lambda_h\nu_n\right)\end{array}\right)\\ +\phi\left(\mu_h+\tau_2\right)l_2\left(kl_1\Lambda_h\nu_n\mathcal{R}_r^0\left(\mathcal{R}_{h_2}^0-1\right)-l_1\Lambda_h\rho_2R_r^0S_{r_{ee}}\left(\mathcal{R}_r^0-1\right)\right)\end{array}\right\},$$

$$b_0 = \frac{\left(\Lambda_h\rho_1l_2+\left(k\nu_n+S_{r_{ee}}\left(\mathcal{R}_r^0-1\right)\rho_2\right)\left(l_1l_2-\phi\tau_1\right)\right)\left(l_2\left(\gamma+\mu_h\right)+\phi\left(\mu_h+\tau_2\right)\right)}{\beta_3\mu_h}.$$

Furthermore, the expression in $b_i's$ are as follows

$$f_1 = l_2S_{r_{ee}}\left(K\left(\left(\mathcal{R}_r^0-1\right)+l_1\right)\nu_n\Lambda_h+\left(\mathcal{R}_r^0-1\right)l_1\left(\left(\mathcal{R}_r^0-1\right)S_{r_{ee}}+S_{h_{fe}}\Lambda_h\right)\rho_2\right),$$

$$f_2 = \left(\mathcal{R}_r^0-1\right)l_2S_{h_{fe}}S_{r_{ee}}\left(K\nu_n\beta_1+\zeta\rho_2+\left(\mathcal{R}_r^0-1\right)S_{r_{ee}}\left(\zeta\Lambda_h+\beta_1\rho_2\right)\right),$$

$$f_3 = \left(\mathcal{R}_r^0-1\right)S_{h_{fe}}S_{r_{ee}}\left(K\nu_n\beta_1+S_{r_{ee}}\left(\left(\mathcal{R}_r^0-1\right)\beta_1+\mathcal{R}_r^0\zeta\rho_2\right)\right).$$

Since, $(l_1l_2-\phi\tau_1) > 0$ here it should be noted that $b_0(<,>)0$, iff $(\mathcal{R}_h^0,\mathcal{R}_r^0)$ $<,>$ 1. Moreover, we summarize the the results as follows.

Theorem 3.3. *[28] Every polynomial equation with an odd degree has at least one real root with a sign opposite to the sign of its last term.*
When $\mathcal{R}_r^0 > 1$ then $b_0 > 0$, and we have two cases:
Case I. When $\mathcal{R}_0 > 1$, then using Theorem 4, Eq (3.8) possesses at least one positive root.
Again two cases arise:
Case II. When $\mathcal{R}_0 > 1$, and if $b_1 < 0, b_2 < 0$ then using Descartes rule of signs, (3.8) has exactly one root with positive sign.
Case III. When $\mathcal{R}_0 > 1$, and if $b_1 > 0, b_2 > 0$ then using Descartes rule of signs, (3.8) has at least one root with positive sign.
Case IV. When $\mathcal{R}_0 \leq 1$, then using Descartes rule of signs Eq (3.8) has no positive root.

3.2.2. Local stability at `MPXFE` point

Theorem 3.4. *The MPX model (2.4) is locally asymptotically stable at `MPXFE` iff $\mathcal{R}_0 < 1$.*

Proof. For the required proof, the necessary condition is that the Jacobian matrix evaluated at $\mathcal{M}_0$ has eigenvalues with negative signs. The subsequent Jacobian matrix $J(\mathcal{M}^0)$ is obtained as

$$J\left(\mathcal{M}^0\right) = \begin{bmatrix} -\mu_h & -\beta_2 & \tau_1 & 0 & -\frac{\mu_r\Lambda_h\beta_1}{\mu_h\Lambda_r} & 0 & -\frac{\Lambda_h\zeta}{K\mu_h} \\ 0 & -l_1+\beta_2 & 0 & 0 & 0 & \frac{\mu_r\Lambda_h\beta_1}{\mu_h\Lambda_r} & \frac{\Lambda_h\zeta}{K\mu_h} \\ 0 & \phi & -l_2 & 0 & 0 & 0 & 0 \\ 0 & \gamma & \tau_2 & -\mu_h & 0 & 0 & 0 \\ 0 & 0 & 0 & 0 & -\mu_r & -\beta_3 & 0 \\ 0 & 0 & 0 & 0 & 0 & -\mu_r+\beta_3 & 0 \\ 0 & \rho_1 & 0 & 0 & 0 & \rho_2 & -\nu_n \end{bmatrix}.$$

The eigenvalues of $J(\mathcal{M}^0)$ are $-\mu_r, -l_2, -\mu_h, -\mu_h$, and $-(-\beta_3+\mu_r)$ and the solution of second degree polynomial can be obtained from $c_0\lambda^2+c_1\lambda+c_2=0$. Here, the coefficients $c_i(i=0,1,2)$ given in terms of $\mathcal{R}_0$ as

$$\begin{aligned} c_0 &= 1, \\ c_1 &= \nu_n + l_1\left(1-\mathcal{R}^0_{h_1}\right), \\ c_2 &= \nu_n l_1\left(1-\mathcal{R}^0_h\right). \end{aligned} \tag{3.9}$$

Since $c_1, c_2 > 0$ if $\mathcal{R}^0_h < 1$, then by Routh-Hurwitz criteria for polynomial of degree two, the system (2.4) is stable locally asymptotically if $\mathcal{R}^0_h < 1$. □

3.2.3. Global stability at `MPXFE` point

Theorem 3.5. *If $\mathcal{R}_0 < 1$ then the `MPXFE` of the proposed model* (2.4) *is globally asymptotically stable (GAS).*

Proof. According to the Castillo Chavez theorem [29], the basic epidemic model can be written as

$$\begin{aligned} X^{'}_{if} &= F\left(X_{if}, Z_{ip}\right), \\ Z^{'}_{ip} &= G\left(X_{if}, Z_{ip}\right), \end{aligned} \tag{3.10}$$

with $G(X_{if},0)=0, X_{if}=(S_h,R_h,S_r)^t$ and $Z_{ip}=(I_h,Q_h,I_r,E_n)^t$. According to the first condition of the theorem, non-infected compartments of MPX epidemic model (2.4) can be shown as

$$\begin{aligned} &X^{'}_{if} = F\left(X_{if},0\right), \\ &\textit{with} \\ &F\left(X_{if},0\right) = \begin{bmatrix} \Lambda_h-\mu_h S_h \\ -\mu_h R_h \\ \Lambda_r-\mu_r S_r \end{bmatrix}. \end{aligned} \tag{3.11}$$

The respective jacobian matrix of $F(X_{if},0)$ is evaluated as

$$J\left(F\left(X_{if},0\right)\right) = \begin{bmatrix} -\mu_h & 0 & 0 \\ 0 & -\mu_h & 0 \\ 0 & 0 & -\mu_r \end{bmatrix}. \tag{3.12}$$

The problem in the system (3.11) will be GAS if $J\left(F\left(X_{if},0\right)\right)$ has negative eigenvalues. Since the eigenvalues of the given matrix (3.12) are clearly negative. Therefore, the system (3.11) is GAS.

By the second condition of the theorem, the infected compartments of the system (2.4) can be written as

$$Z_{ip}^{'} = AZ_{ip} - \bar{G}\left(X_{if}, Z_{ip}\right), \tag{3.13}$$

where,

$$A = \begin{bmatrix} -l_1+\beta_2 & 0 & \frac{\beta_1\Lambda_h\mu_r}{\Lambda_r\mu_h} & \frac{\zeta\Lambda_h}{k\mu_h} \\ \phi & -l_2 & 0 & 0 \\ 0 & 0 & \beta_3-\mu_r & 0 \\ \rho_1 & 0 & \rho_2 & -\nu_n \end{bmatrix}, \text{ and}$$

$$\bar{G}\left(X_{if}, Z_{ip}\right) = \begin{bmatrix} \beta_1 I_r\left(\frac{S_h^0}{N_{r0}} - \frac{S_h}{N_r}\right) + \beta_2 I_h\left(\frac{S_h^0}{N_h^0} - \frac{S_h}{N_h}\right) + \zeta E_n\left(\frac{S_h^0}{k} - \frac{S_h}{k+E_n}\right) \\ 0 \\ \beta_3 I_r\left(1 - \frac{S_r}{N_r}\right) \\ 0 \end{bmatrix}.$$

Clearly, $\bar{G}(X_{if}, Z_{ip}) \geq 0$, since $\frac{S_h^0}{N_r^0} \geq \frac{S_h}{N_r}$, $\frac{S_h^0}{N_h^0} \geq \frac{S_h}{N_h}$, and $\frac{S_h^0}{k} - \frac{S_h}{k+E_n} = \frac{S_h^0 E_n + \left(S_h^0 - S_h\right)k}{k(k+E_n)} \geq 0$. Therefore, the Eq (3.13) becomes

$$Z_{ip}^{'} \leq AZ_{ip},$$

where the eigenvalues are $-l_2, \mu_r\left(\mathcal{R}_r^0 - 1\right)$, and the solution of the polynomial equation

$$c_0\lambda^2 + c_1\lambda + c_2 = 0, \tag{3.14}$$

where, $c_i, i = 0, 1, 2$ are given below

$$\begin{aligned} c_2 &= l_1\nu_n\left(1 - \mathcal{R}_h^0\right), \\ c_1 &= l_1\left(1 - \mathcal{R}_{h_1}^0\right), \\ c_0 &= 1. \end{aligned} \tag{3.15}$$

Clearly, (3.14) has negative eigenvalues and therefore, the matrix A satisfies the second condition of the comparison theorem. Thus, the `MPXFE` point is GAS if $\mathcal{R}_h^0 < 1$ otherwise unstable. □

4. Sensitivity analysis

Sensitivity analysis is a strong tool that helps in identifying the significantly influential factor on the reproductive number. Moreover, this analysis is useful to set a suitable optimal control intervention for disease minimization. Due to possible errors in data collection and the assumed parameters, the sensitivity analysis determines the robustness of the model prediction to the variation of parameters values. In this regard, various approaches have been applied in the literature. In this study, we utilized

the parametric approach of the normalized forward sensitivity indices introduced in [30]. A positive (or negative) index value indicates that the corresponding parameter directly (inversely) affects $\mathcal{R}_0$. The formulae for the normalized forward sensitivity index for the model key parameters is defined as follows:

Definition 4.1. *The aforementioned technique to measure the relative change in $\mathcal{R}_0$ with respect to the relative change in the model parameter say x is given by [30]:*

$$Y_x = \frac{x}{|\mathcal{R}_0|} \times \frac{\partial \mathcal{R}_0}{\partial x}. \tag{4.1}$$

Further, using the formula stated in (4.1), we evaluate the respective indices of various model parameters. These indices are given in Table 2. The parameters having considerable impact on $\mathcal{R}_r^0$ and $\mathcal{R}_h^0$ are $\beta_3, \mu_r, \beta_2, \zeta, \Lambda_h, \rho_1, \mu_h, \nu_n, K, \gamma, \delta$, and ϕ. The respective expressions evaluated by the formula mentioned above are given below. Because of their sensitivity indices, these factors identify potential preventive strategies. The following expressions are obtained for different parameters using the formula defined in (4.1)

$$Y_{\beta_3} = 1,\ Y_{\mu_r} = -1,$$

$$Y_{\beta_2} = \frac{\mathcal{R}_{h_1}}{\mathcal{R}_h},$$

$$Y_\zeta = Y_{\rho_1} = \frac{\mathcal{R}_{h_2}}{\mathcal{R}_h},$$

$$Y_K = Y_{\nu_n} = -\frac{\mathcal{R}_{h_2}}{\mathcal{R}_h},$$

$$Y_{\mu_h} = -\frac{\mu_h\left(\frac{\mathcal{R}_h}{l_1} + \frac{\mathcal{R}_{h_2}}{\mu_h}\right)}{\mathcal{R}_h},$$

$$Y_\gamma = \frac{-\gamma}{l_1},\quad Y_\delta = \frac{-\delta}{l_1},$$

$$Y_\phi = -\frac{\phi}{l_1},$$

where, $Y_{\beta_3}, Y_{\mu_r}, Y_{\beta_2}, Y_\zeta, Y_{\rho_1}, Y_K, Y_{\nu_n}, Y_{\mu_h}, Y_\gamma, Y_\delta$, and Y_ϕ denote the normalizer of sensitivity index with respect to $\beta_3, \mu_r, \beta_2, \zeta, \rho_1, K, \nu_n, \mu_h, \gamma, \delta$, and ϕ, respectively. The corresponding numerical normalized sensitivity indices using the estimated parameters are given in Table 2, while the bar plot is depicted in Figure 3. It is observed that some of the parameters have positive signs and some have negative signs with indices. The parameters with positive indices directly relate to the basic reproduction number, which means that the reduction in these parameters reducesthe disease incidence. On the other hand, the parameters with negative indices have an inverse relation with reproduction numbers, revealing that enchasing these parameters will reduce the disease rate. Based on the sensitivity indices mentioned in the table below, the feasible and effective optimal control interventions are the use of personal protection (capable of reducing $\beta_1, \beta_2, \beta_3$, ζ), proper contact tracing and isolation policy (enhancing ϕ), reducing the shedding rate of infection in the environment (reducing ρ_1, ρ_2), and fumigating commercial areas (increasing the virus decay in the environment i.e., ν_n).

Table 2. Sensitivity analysis.

Symbols	Sensitivity index of $\mathcal{R}_h^0$	Sensitivity index of $\mathcal{R}_r^0$
β_3		+1.0000
μ_r		−1.0000
β_2	+0.0698	
μ_h	−0.9302	
ρ_1	+0.9302	
γ	−0.3245	
ν_n	−0.9302	
δ	−0.3219	
ζ	+0.9302	
ϕ	−0.4534	
Λ_h	+0.9302	
k	−0.9302	

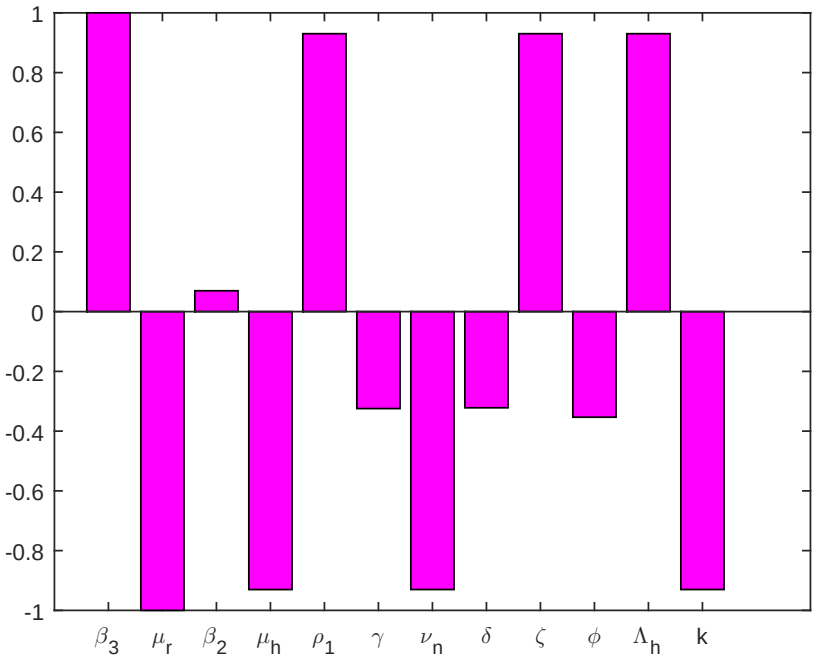

Figure 3. Bar graph of sensitivity indices of MPX model.

5. Optimal control analysis

This part presents the formulation of a control problem to suggest the optimized control intervention to reduce the disease incidence within a community. Moreover, this section includes the existence criteria and solution of the proposed control system. Based on normalized sensitivity indices, we construct an optimum control system by incorporating six time-dependent controls in the MPX

model (2.4). The time-dependent control measures are represented by u_1, u_2, u_3, u_4, u_5, and u_6 with the details and biological meaning as follows:

- u_1: use of personal protections minimizing infection transmission to susceptible humans from infected humans and animals
- u_2: use personal protections minimizing infection transmission to susceptible humans from environmental routes (i.e., cleaning of contaminated surfaces/environment with home-based detergents, etc.)
- u_3: isolation via contact tracing
- u_4: use of protections measures minimizing infection transmission between susceptible and infected animals
- u_5: 5^{th} control measure used for reducing the shedding rate of infection in the environment
- u_6: 6^{th} fumigating commercial areas to increase the MPXV decay rate in the environment

With the use of the aforementioned controls, this part seeks to build an optimal control problem to explain how the variable control problem contributes to the eradication of the disease. The developed control problem is given in (5.1).

$$\begin{aligned}
\frac{dS_h}{dt} &= \Lambda_h - \left(\frac{\beta_1 I_r}{N_r} + \frac{\beta_2 I_h}{N_h}\right) S_h(1-u_1(t)) - \frac{\zeta E_n S_h}{K+E_n}(1-u_1(t)-u_2(t)) + \tau_1 Q_h - \mu_h S_h,\\
\frac{dI_h}{dt} &= \left(\frac{\beta_1 I_r}{N_r} + \frac{\beta_2 I_h}{N_h}\right) S_h(1-u_1(t)) + \frac{\zeta E_n S_h}{K+E_n}(1-u_1(t)-u_2(t)) - (u_3+\gamma+\mu_h+\delta) I_h,\\
\frac{dQ_h}{dt} &= u_3 I_h - (\tau_1+\tau_2+\mu_h) Q_h,\\
\frac{dR_h}{dt} &= \gamma I_h + \tau_2 Q_h - \mu R_h,\\
\frac{dS_r}{dt} &= \Lambda_r - \frac{\beta_3 I_r S_r}{N_r}(1-u_4) - \mu_r S_r,\\
\frac{dI_r}{dt} &= \frac{\beta_3 I_r S_r}{N_r}(1-u_4) - \mu_r I_r,\\
\frac{dE_n}{dt} &= (1-u_5)\rho_1 I_H + (1-u_5)\rho_2 I_r - (u_6+\nu_n) E_n,
\end{aligned} \tag{5.1}$$

subject to initial conditions as in (2.5). The objective functional corresponding to the above control system is described as

$$J(u_1,u_2,u_3,u_4,u_5,u_6) = \int_0^T \left(\begin{array}{l} (\mathcal{A}_1 I_h + \mathcal{A}_2 Q_h + \mathcal{A}_3 I_r + \mathcal{A}_4 E_n) + \frac{1}{2} \\ \left(\mathcal{B}_1 u_1^2 + \mathcal{B}_2 u_2^2 + \mathcal{B}_3 u_3^2 + \mathcal{B}_4 u_4^2 + \mathcal{B}_5 u_5^2 + \mathcal{B}_6 u_6^2\right) \end{array} \right) dt. \tag{5.2}$$

While $\mathcal{A}_1, \mathcal{A}_2, \mathcal{A}_3, \mathcal{A}_4$ are the associated balancing constants, $\mathcal{B}_1, \mathcal{B}_2, \mathcal{B}_3, \mathcal{B}_4, \mathcal{B}_5, \mathcal{B}_6$ represents the associated cost factors, and T represents the final step size. Our main objective is to seek optimal controls $u_1^*, u_2^*, u_3^*, u_4^*, u_5^*$, and u_6^*, so that

$$J(u_1^*, u_2^*, u_3^*, u_4^*, u_5^*, u_6^*) = \min_{\Xi} \{J(u_1,u_2,u_3,u_4,u_5,u_6)\},$$

with the control set corresponds to above is given by

$$\Xi = \{(u_1, u_2, u_3, u_4, u_5, u_6) : [0, T] \to [0, 1] \ \ (u_1, u_2, u_3, u_4, u_5, u_6) \ \ is\, a\, Lebesgue\, measurable\}. \quad (5.3)$$

5.1. Existence of the problem

Here, we demonstrate the existence of the optimized control MPX problem (5.1). To obtain the desired outcome, we employ the methodology established in [31, 32]. The problem in (5.1) comprised bounded equations, and if the subsequent conditions are met, the outcomes provided in [31, 32] can be utilized to address the existence of the control problem under consideration:

(1) The control set Ξ and model state variables are not empty as defined earlier.
(2) The control variables represented by Ξ form a closed and convex set.
(3) One can notice that every equation situated on the right-hand side of the control system (5.1) represents a continuous function that has an upper bound equivalent to the total of the bounded control and state variables. Additionally, these equations can be written as a linear function of u, with coefficients that rely on the time and state variables.
(4) There exist some constants $\zeta_1 > 0$, $\zeta_2 > 0$, and $q > 1$, so that the integrand involved in the objective functional $\mathcal{J}$ given by (5.2) is convex and fulfills the inequality stated below:

$$\mathcal{F}(y, u, t) \geq \zeta_1(|u_1|^2 + |u_2|^2 + |u_3|^2 + |u_4|^2 + |u_5|^2 + |u_6|^2)^{\frac{p}{2}} - \zeta_2.$$

The approach established in [31, 32] easily satisfies the aforementioned conditions 1 to 4. The first two conditions are evident as as the state variables and controls are both nonempty and bounded, resulting in solutions that are also convex and bounded. Additionally, it can be seen that the third condition is fulfilled due to the fact that the system is bilinear in control variables. Furthermore, the bilinearity of the system in control variables satisfies Condition 3. Finally, to assess Condition 4, one can conveniently write:

$$\begin{aligned}\mathcal{A}_1 I_h + \mathcal{A}_2 Q_h + \mathcal{A}_3 I_r + \mathcal{A}_4 E_n + 1/2\left(\mathcal{B}_1 u_1^2 + \mathcal{B}_2 u_2^2 + \mathcal{B}_3 u_3^2 + \mathcal{B}_4 u_4^2 + \mathcal{B}_5 u_5^2 + \mathcal{B}_6 u_6^2\right) \\ \geq \zeta_1(|u_1|^2 + |u_2|^2 + |u_3|^2 + |u_4|^2 + |u_5|^2 + |u_6|^2)^{\frac{p}{2}} - \zeta_2.\end{aligned}$$

Thus, we state the following theorem for the optimal control problem existence.

Theorem 5.1. *The optimal control set shown by* $u^* = \left(u_1^*, u_2^*, u_3^*, u_4^*, u_5^*, u_6^*\right)$ *exists if the objective functional* $\mathcal{J}$ *over the control set* Ξ *corresponding to (5.1) fulfills the conditions (1–4) stated above. Furthermore, we have*

$$\mathcal{J}\left(u_1^*, u_2^*, u_3^*, u_4^*, u_5^*, u_6^*\right) = \min_{\Xi}\left\{J\left(u_1, u_2, u_3, u_4, u_5, u_6\right)\right\}.$$

5.1.1. Solution of control problem

This section analyzes the solution to the optimal control problem for the MPX model dynamics considered in (5.1). The well-known Pontryagin's maximum principle [33] is used for this purpose. The required optimal solution is represented by $\left(u_1^*, u_2^*, u_3^*, u_4^*, u_5^*, u_6^*\right)$. Furthermore, for the necessary

optimal conditions utilized in the finding the solution, we need Lagrangian and Hamiltonian, which are stated as follows

$$L = (\mathcal{A}_1 I_h + \mathcal{A}_2 Q_h + \mathcal{A}_3 I_r + \mathcal{A}_4 E_n) + \frac{1}{2}\left(\mathcal{B}_1 u_1^2 + \mathcal{B}_2 u_2^2 + \mathcal{B}_3 u_3^2 + \mathcal{B}_4 u_4^2 + \mathcal{B}_5 u_5^2 + \mathcal{B}_6 u_6^2\right), \tag{5.4}$$

and

$$\begin{aligned}
\mathbb{H} =& \mathcal{A}_1 I_h + \mathcal{A}_2 Q_h + \mathcal{A}_3 I_r + \mathcal{A}_4 E_n + \frac{1}{2}(\mathcal{B}_1 k_1^2 + \mathcal{B}_2 k_2^2 + \mathcal{B}_3 k_3^2 + \mathcal{B}_4 k_4^2 + \mathcal{B}_5 k_5^2 + \mathcal{B}_6 k_6^2) \\
&+ h_1\left\{\Lambda_h - \left(\frac{\beta_1 I_r}{N_r} + \frac{\beta_2 I_h}{N_h}\right) S_h(1 - u_1(t)) - \frac{\zeta E_n S_h}{K + E_n}(1 - u_1(t) - u_2(t)) + \tau_1 Q_h - \mu_h S_h\right\} \\
&+ h_2\left\{\left(\frac{\beta_1 I_r}{N_r} + \frac{\beta_2 I_h}{N_h}\right) S_h(1 - u_1(t)) + \frac{\zeta E_n S_h}{K + E_n}(1 - u_1(t) - u_2(t)) - (u_3 + \gamma + \mu_h + \delta) I_h\right\} \\
&+ h_3\{u_3 I_h - (\tau_1 + \tau_2 + \mu_h) Q_h\} + h_4\left\{\gamma I_h + \tau_2 Q_h - \mu_h R_h\right\} + h_5\left\{\Lambda_r - \frac{\beta_3 I_r S_r}{N_r}(1 - u_4) - \mu_h S_r\right\} \\
&+ h_6\left\{\frac{\beta_3 I_r S_r}{N_r}(1 - u_4) - \mu_h I_r\right\} + h_7\left\{(1 - h_5)\rho_1 I_h + (1 - h_5)\rho_2 I_r - (u_6 + \nu_n) E_n\right\},
\end{aligned} \tag{5.5}$$

where, $h_i, i = 1, 2, ..., 7$ demonstrates the adjoint variables.

$$\begin{cases}
\frac{dz}{dt} = \frac{\partial}{\partial h_i}\mathbb{H}\left(t, u_j^*, h_i\right), \\
\frac{\partial}{\partial k}\mathbb{H}\left(t, u_j^*, h_i\right) = 0, \\
\frac{dh_i(t)}{dt} = -\frac{\partial}{\partial z} h_i\left(t, u_j^*, h_i\right).
\end{cases} \tag{5.6}$$

The criteria stated in (5.6) with the theorem given below have been used to attain the solution of the optimum problem.

Theorem 5.2. *If the controls* $\left(u_1^*, u_2^*, u_3^*, u_4^*, u_5^*, u_6^*\right)$ *and the solution* $\left(S_h^*, I_h^*, Q_h^*, R_h^*, S_r^*, I_r^*, E_n^*\right)$ *of the corresponding control problem (5.1) minimizes the objective function in the problem, then there exist an adjoint variables (co-state variables)* $h_i, i = 1, 2, ..., 7$ *further the corresponding transversality*

conditions $h_i(T) = 0, \;\; i = 1, 2, 3.....7$, *such that*

$$
\begin{aligned}
h_1'(t) &= (h_2 - h_1)\frac{\beta_2 S_h^* I_h^*}{(N_h^*)^2} + (h_1 - h_2)\left(\left(\frac{\beta_1 I_r^*}{N_r^*} + \frac{\beta_2 I_h^*}{N_h^*}\right)(1 - u_1) + \frac{\zeta E_n^*(1-u_1-u_2)}{k+E_n^*}\right) + h_1\mu_h,\\
h_2'(t) &= -\mathcal{A}_1 - \gamma h_4 - h_3 u_3 + (h_2 - h_1)(1 - u_1)\frac{\beta_2 S_h^* I_h^*}{(N_h^*)^2} + (h_1 - h_2)(1 - u_1)\frac{\beta_2 S_h^*}{N_h^*} + h_2\\
&\quad + h_2(\gamma + \delta + \mu_h + u_3) - h_7(1 - u_5)\rho_1,\\
h_3'(t) &= -\mathcal{A}_2 + (h_2 - h_1)(1 - u_1)\frac{\beta_2 S_h^* I_h^*}{(N_h^*)^2} + (h_3 - h_1)\tau_1 + (h_3 - h_4)\tau_2 + \mu_h h_3,\\
h_4'(t) &= (h_2 - h_1)(1 - u_1)\frac{\beta_2 S_h^* I_h^*}{(N_h^*)^2} + \mu_h h_4,\\
h_5'(t) &= (h_2 - h_1)(1 - u_1)\frac{\beta_1 S_h^* I_r^*}{(N_r^*)^2} + (h_5 - h_6)(1 - u_4)\frac{\beta_1 I_r^*(N_r^* - S_r^*)}{(N_r^*)^2} + \mu_r h_5,\\
h_6'(t) &= -\mathcal{A}_3 + (h_2 - h_1)(1 - u_1)\frac{\beta_1 S_h^* I_r^*}{(N_r^*)^2} + (h_1 - h_2)(1 - u_4)\frac{\beta_1 S_h^*}{N_r^*} + (h_6 - h_5)(1 - u_4)\\
&\quad \times\frac{\beta_1 I_r^* S_r^*}{(N_r^*)^2} + (h_5 - h_6)(1 - u_4)\frac{\beta_1 S_r^*}{N_r^*} - h_7(1 - u_5)\rho_2 + \mu_r h_6,\\
h_7'(t) &= -\mathcal{A}_4 + h_7(u_6 + \nu_n) + (h_2 - h_1)\frac{\zeta E_n^* S_h^*(1-u_1-u_2)}{(k+E_n^*)^2} + (h_1 - h_2)\frac{\zeta S_h^*(1-u_1-u_2)}{(k+E_n^*)}.
\end{aligned}
\tag{5.7}
$$

Moreover, we obtain the optimum controls $\left(u_1^*, u_2^*, u_3^*, u_4^*, u_5^*, u_6^*\right)$ *which minimizes the problem over the region* Ξ *as follows*

$$
\begin{aligned}
&u_1^* = \min\left(\max\left(0, \bar{u}_1\right), 1\right), \;\; u_2^* = \min\left(\max\left(0, \bar{u}_2\right), 1\right), \;\; u_3^* = \min\left(\max\left(0, \bar{u}_3\right), 1\right),\\
&u_4^* = \min\left(\max\left(0, \bar{u}_4\right), 1\right), \;\; u_5^* = \min\left(\max\left(0, \bar{u}_5\right), 1\right), \;\; u_6^* = \min\left(\max\left(0, \bar{u}_6\right), 1\right),\\
&\textit{where},\\
&\bar{u}_1 = \frac{(h_2-h_1)S_h^*}{\mathcal{B}_1}\left(\left(\frac{\beta_1 I_r^*}{N_r^*} + \frac{\beta_2 I_h^*}{N_h^*}\right) + \frac{\zeta E_n^*}{k+E_n^*}\right), \;\; \bar{u}_2 = \frac{(h_2-h_1)S_h^*}{\mathcal{B}_2}\left(\frac{\zeta E_n^*}{k+E_n^*}\right), \;\; \bar{u}_3 = \frac{(h_2-h_3)I_h^*}{\mathcal{B}_3},\\
&\bar{u}_4 = \frac{(h_6-h_5)\beta_3 S_r^* I_r^*}{\mathcal{B}_4 N_r^*}, \;\; \bar{u}_5 = \frac{h_7\left(\rho_1 I_h^* + I_r^*\rho_2\right)}{\mathcal{B}_5}, \;\; \textit{and} \;\; \bar{u}_6 = \frac{h_7 E_n^*}{\mathcal{B}_6}.
\end{aligned}
\tag{5.8}
$$

Proof. By utilizing the conditioned mentioned in (5.6), and the transversilty conditions,the results given in (5.7) are obtained for (5.5) by setting $S_h = S_h^*, I_h = I_h^*, Q_h = Q_h^*, S_r = S_r^*, I_r = I_r^*$ and $E_n = E_n^*$. Furthermore, using the condition $\frac{\partial}{\partial k}H\left(t, \breve{k}_j, h_i\right) = 0$ for $j = 1, 2, ...6$ and $i = 1, 2, ...7$ given in (5.6),the optimal control in (5.7) are obtained. □

6. Simulation and discussion of the control MPX problem

Here, we focus to demonstrate the numerical simulation of the MPX model with and without optimized control interventions to analyze the impact of control variables introduced in the previous

section. The numerical solution of the control problem (5.1) and the corresponding adjoint control system is carried out by employing the backward fourth-order Runge-Kutta. The initial conditions for the state variables in section 2 and the values of the model parameters are given in Table 1. Most of the parameters are esteemed from reported cases during the 2022 outbreak and some are taken from literature.

Four different optimized predictive control strategies are developed to illustrate their impact on the infection incidence in a community. The following combination of control variables constructs four control strategies, namely A, B, C, and D:

- Strategy A: consist of a combination of all control measures.
- Strategy B: combination of u_3, u_5 and u_6 control variables only. In this case, we ignore the use of personal protection controls.
- Strategy C: using all control variables except the isolation control u_3.
- Strategy D: using all control variables except u_5 and u_6.

The detailed simulation along with a discussion of the above four interventions are given in the following subparts.

6.1. Strategy A: using all the control variables

In this case, the MPX control problem (5.1) is simulated by activating all control variables $u_1, u_2, u_3, u_4, u_5, u_6$. This means that all interventions mentioned in the previous section are applied simultaneously. The simulation corresponding to the present strategy for human and animal populations are illustrated in Figure 4(a–d) and Figure 5(a,b) respectively. The profiles of all optimal control variables are shown in Figure 5(c). Figure 4(a) demonstrates the dynamics of susceptible human individuals under the application of all control interventions. The population in this class increases with the application of the optimal controls. Figure 4(b) shows the dynamics of solution trajectories of the infected MPX human population. It can be observed that without optimal controls, the population of infected humans raised quickly. However, with application of the suggested optimal controls, the infected population vanishes. Figure 4(c) describes the impact of using all control variables on the population of the isolated class. As the controls act quickly from the onset of the application, the isolated population increased significantly. On the other hand, without controls, the isolated population decreased and reached zero. This shows the efficacy of effective contact tracing and isolation the infected population. Figure 4(d) describes the dynamics of the recovered human population with and without optimal control variables. The recovered population decreases with the application of control measures. By applying effective preventive controls, fewer people will acquire infection, and as a result, fewer individuals recover from the infection. The dynamics of susceptible and infected animals are analyzed in Figures 5(a,b), respectively. In Figure 5(a), we observed that the population of susceptible animals was almost the same with and without optimal controls. Howsoever, the number of infected animals significantly decreases under the application of all control interventions and reaches zero after 70 days. Figure 5(c) shows the concentration of the MPXV in the environment. The application of optimal controls effectively decreased the viral concentration level in the environment compared to the case without optimal controls. Figure 6(a–f) illustrates the control profiles of all control variables, showing their level of application over considered time intervals.

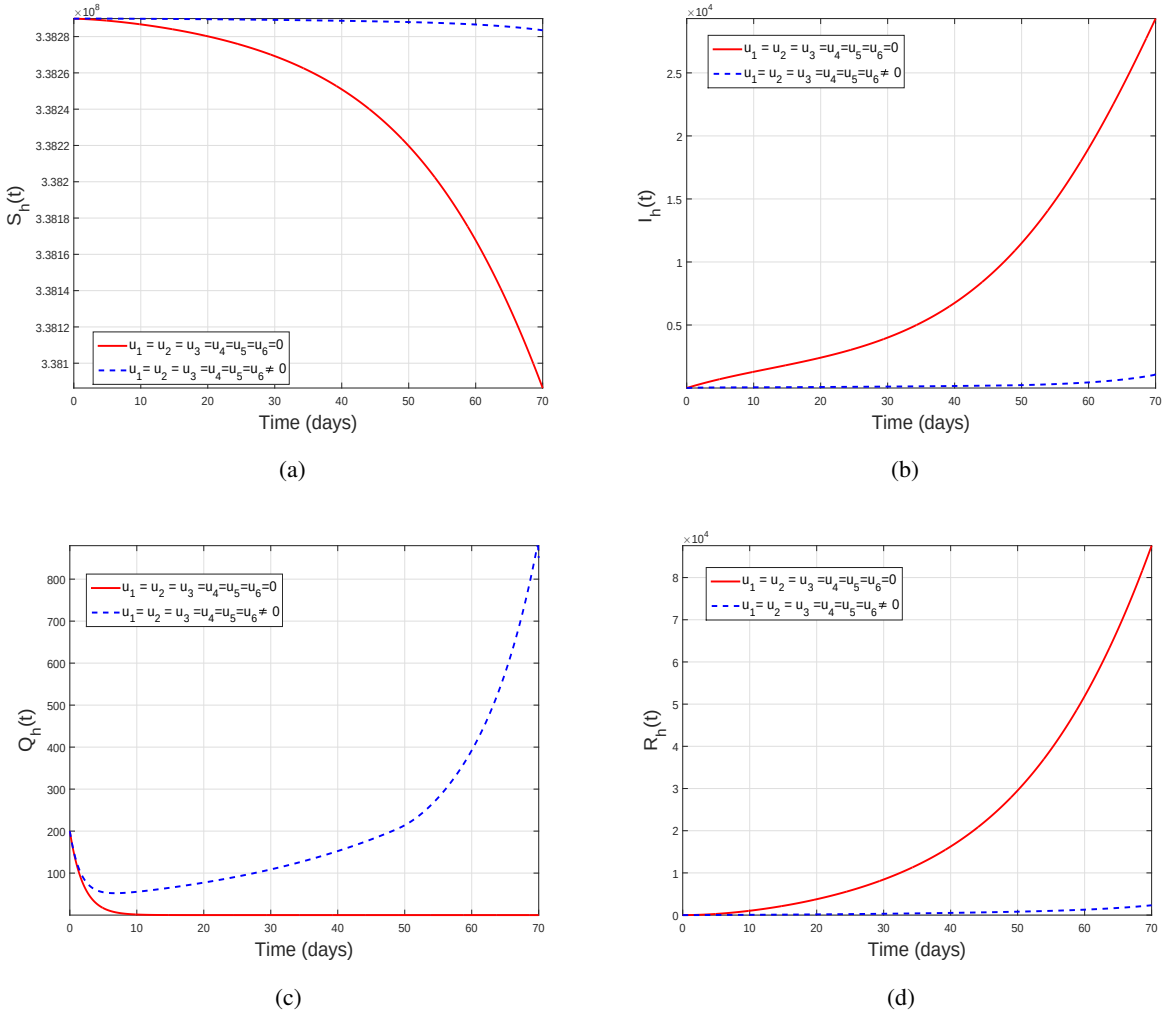

Figure 4. Simulation of the MPX control model (5.1) with considering all control variables i.e., $u_1 \neq 0$, $u_2 \neq 0$, $u_3 \neq 0$, $u_4 \neq 0$, $u_5 \neq 0$, and $u_6 \neq 0$. The dashed blue curves show the simulation with controls and the solid red curves shows the simulation without optimal controls. (a) Susceptible human. (b) Infected human. (c) Isolated human. (d) Recovered human.

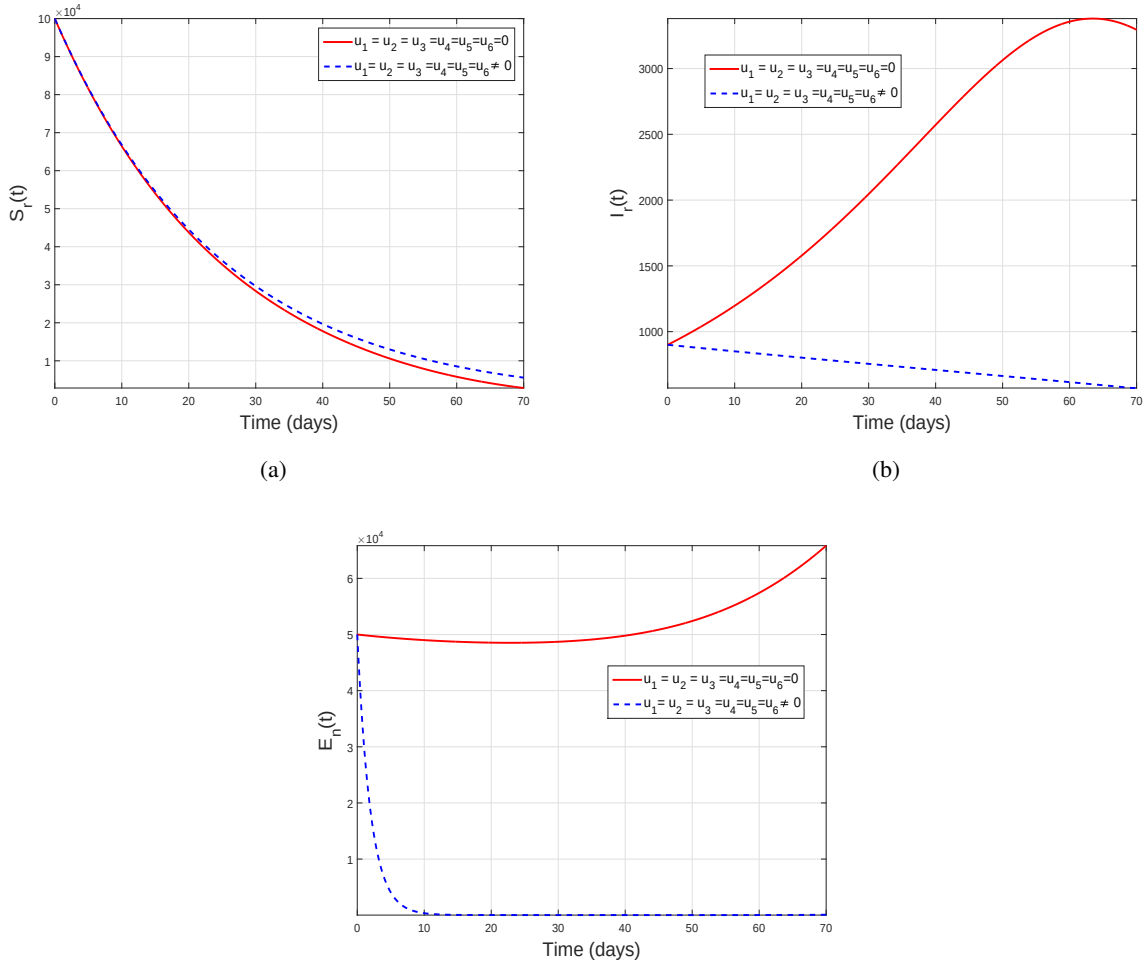

Figure 5. Simulation of the MPX control model (5.1) with considering all control variables i.e., $u_1 \neq 0$, $u_2 \neq 0$, $u_3 \neq 0$, $u_4 \neq 0$, $u_5 \neq 0$, and $u_6 \neq 0$. The dashed blue curves show the simulation with controls and the solid red curves shows the simulation without optimal controls. (a) Susceptible animals. (b) Infected animals. (c) Environmental viral concentration.

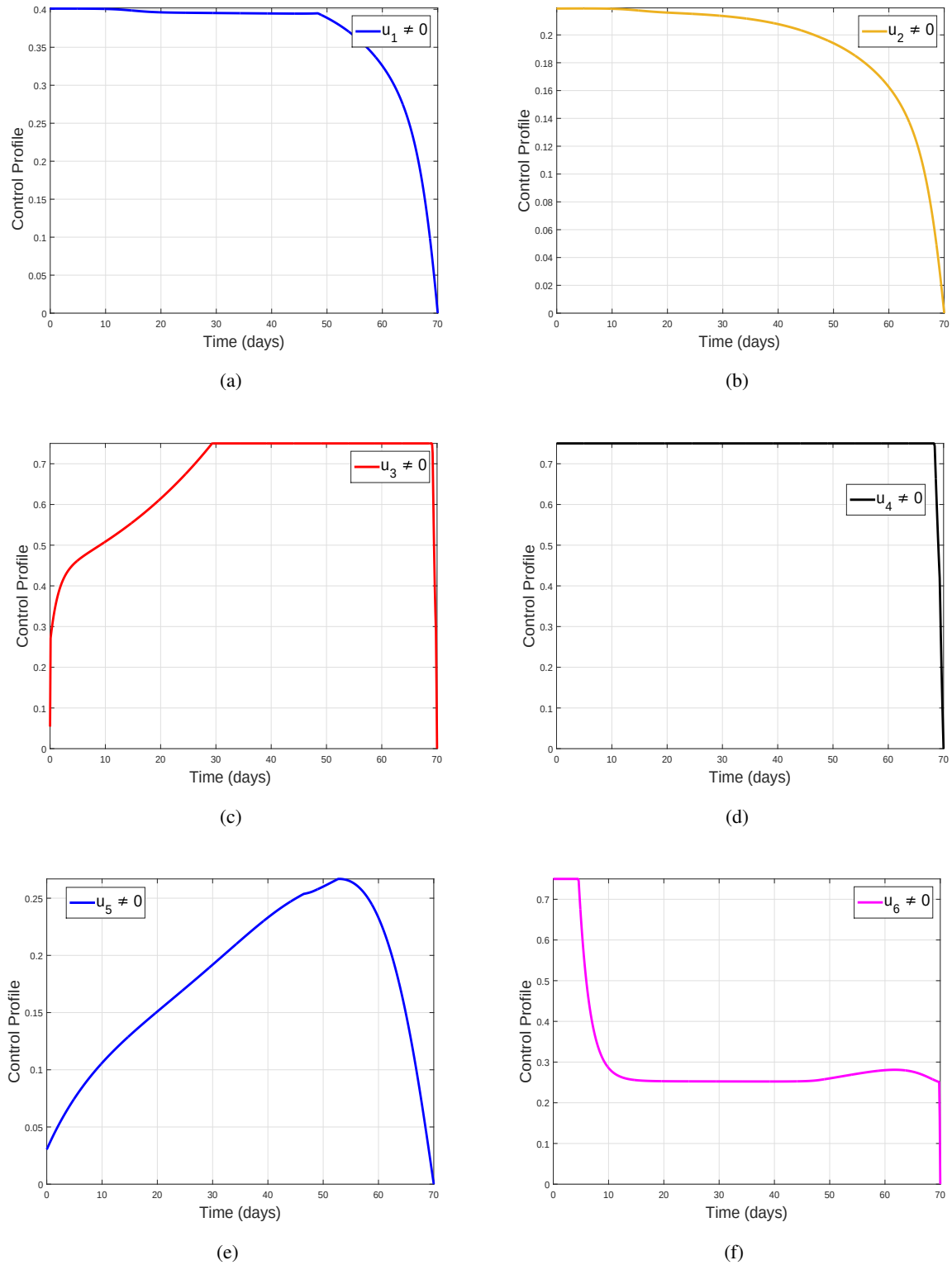

Figure 6. The corresponding control profile for strategy A. (a) u_1, (b) u_2, (c) u_3, (d) u_4, (e) u_5, (f) u_6.

6.2. *Strategy B: using u_3, u_5 and u_6 control variables only*

This strategy analyzes the combined impact of control measures u_3, u_5, and u_6 and sets the rest as zero (i.e., $u_1 = u_2 = u_4 = 0$). This means that the use of personal protection measures for both human and animal populations is not consideredin this case. Simulation of strategy B with control profiles are shown in Figures 7–9. This strategy is less useful for disease eradication although the infected human population decreases with the application of optimal controls as can be seen in Figure 7(b). The population in the isolated class raises quickly with control compared to without control application, as seen in Figure 7(c). Further, this strategy has no impact on the dynamics of the animal population, as seen in Figure 8(a,b). The concentration of the MPX virus in the environmentsignificantly reduces as the controls act quickly from the onset of the application, as seen in Figure 8(c). Figure 9(a–f) shows the control profiles corresponding to strategy B. Overall, it is clear that without personal protection measures, the infection can not be curtailedeffectively.

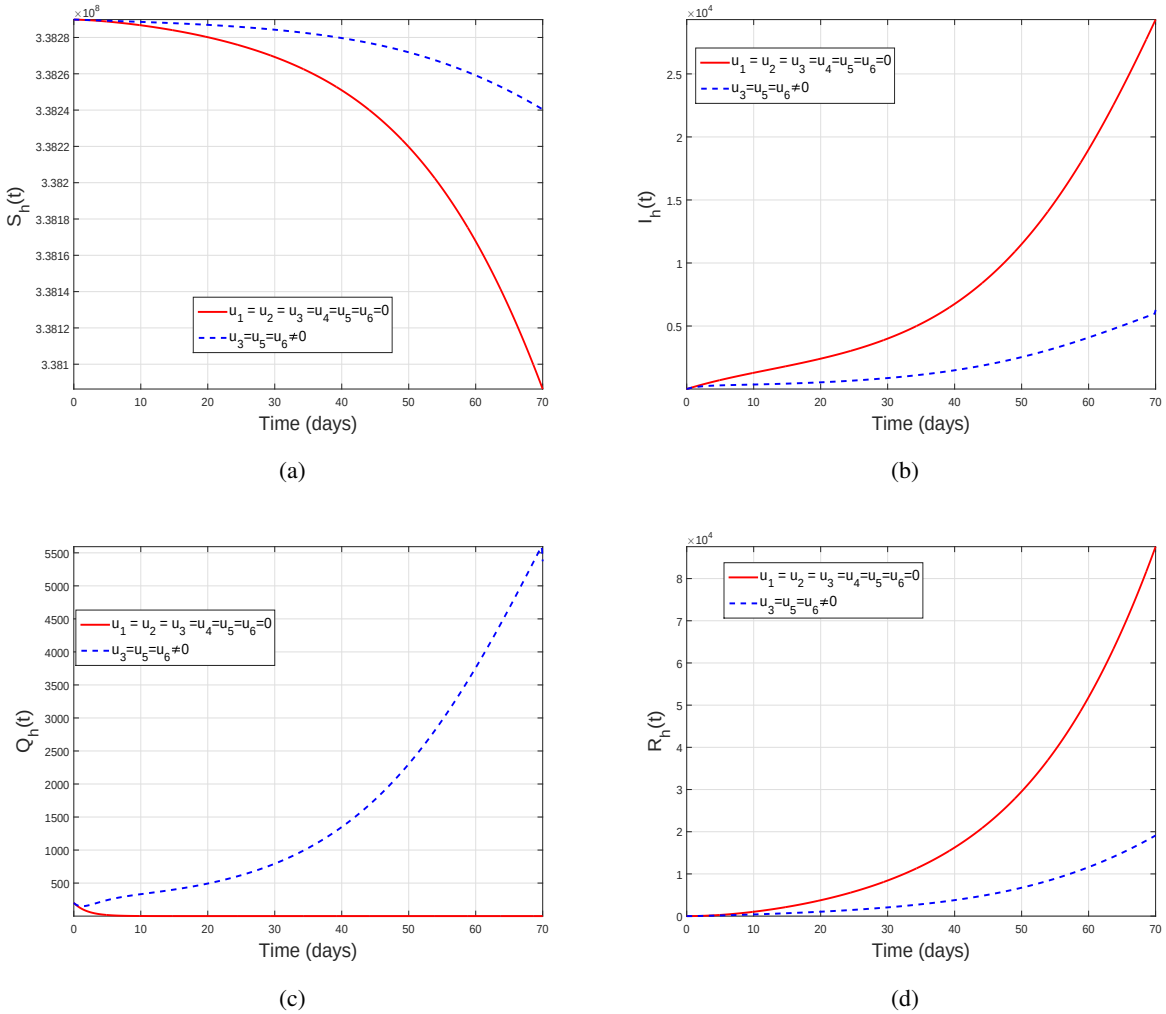

Figure 7. Simulation of the MPX control model (5.1) using u_3, u_5, and u_6 control variables only. (a) Susceptible human. (b) Infected human. (c) Isolated human. (d) Recovered human.

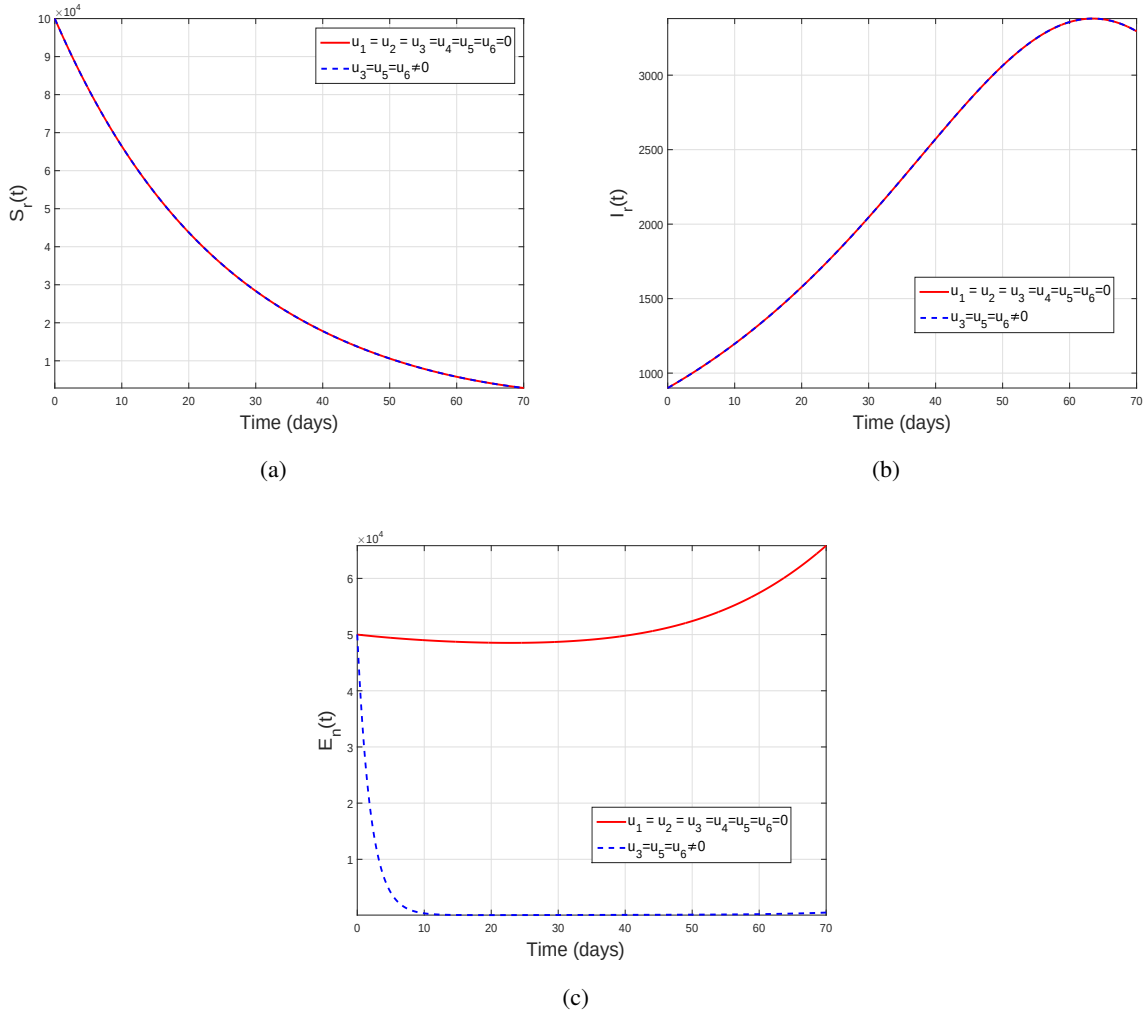

Figure 8. Simulation of the MPX control model (5.1) using u_3, u_5, and u_6 control variables only. (a) Susceptible animals. (b) Infected animals. (c) Environmental viral concentration.

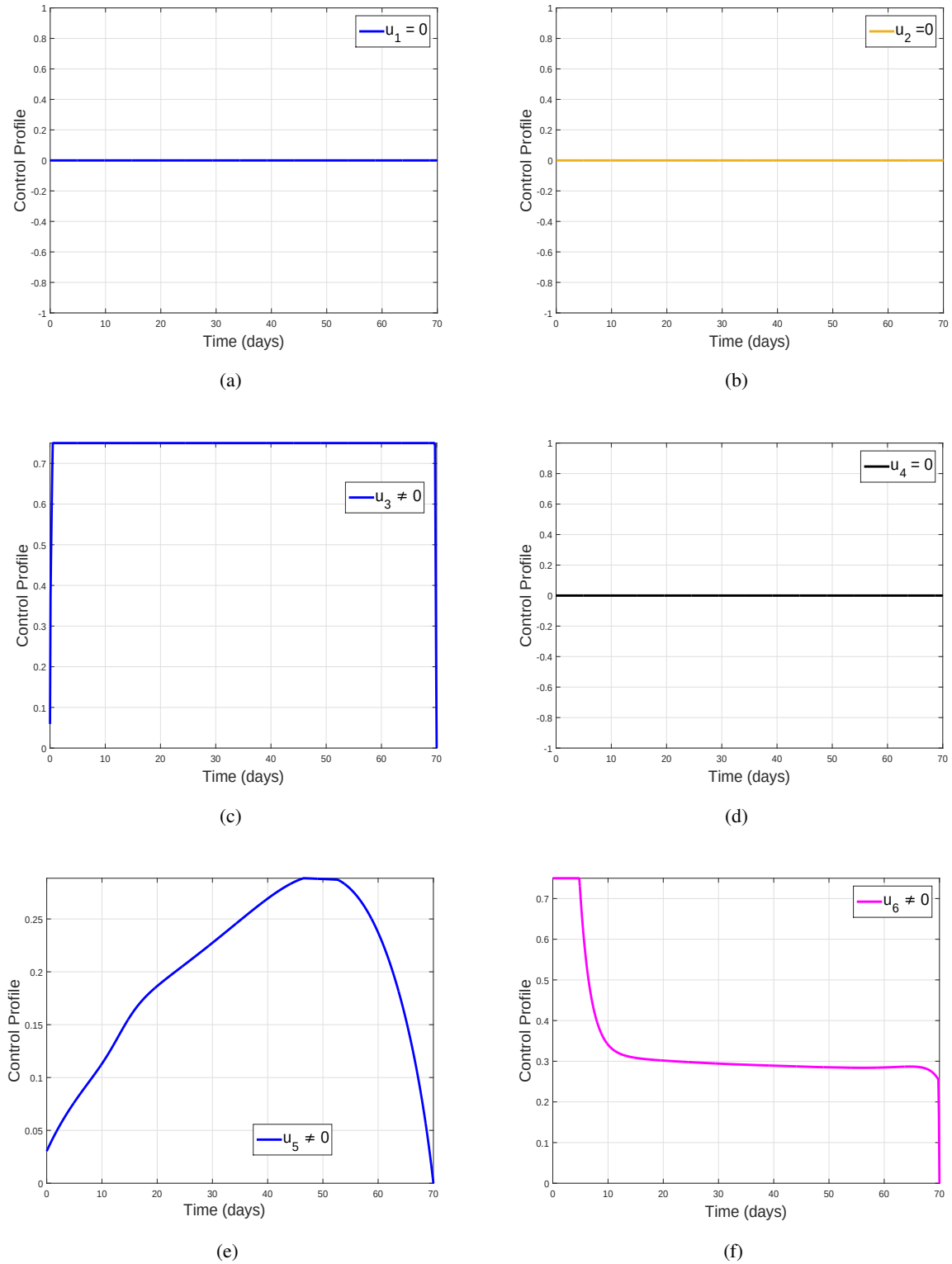

Figure 9. The corresponding control profile for strategy B. (a) u_1, (b) u_2, (c) u_3, (d) u_4, (e) u_5, (f) u_6.

6.3. *Strategy C: using all control variables except the isolation control u_3.*

Strategy C describes the impact of all control variables, except for the isolation control u_3 on the disease dynamics. The simulation of human and animal populations in this case is depicted in Figure 10(a–d) and Figure 11(a,b), respectively. The concentration of the virus in the environment is depicted in Figure 11(c). The control profiles of all control variables in strategy C are analyzed in Figure 12(a–f). Since no isolation policy is utilized, the population in isolated classes decreases in both with and without cases. However, it is observed that the individuals in the infected human class declined quickly with the application of optimal controls as compared to the without control case. Although, the reduction in infected human individuals is comparatively slower than strategy A, though it can be used for disease eradication.

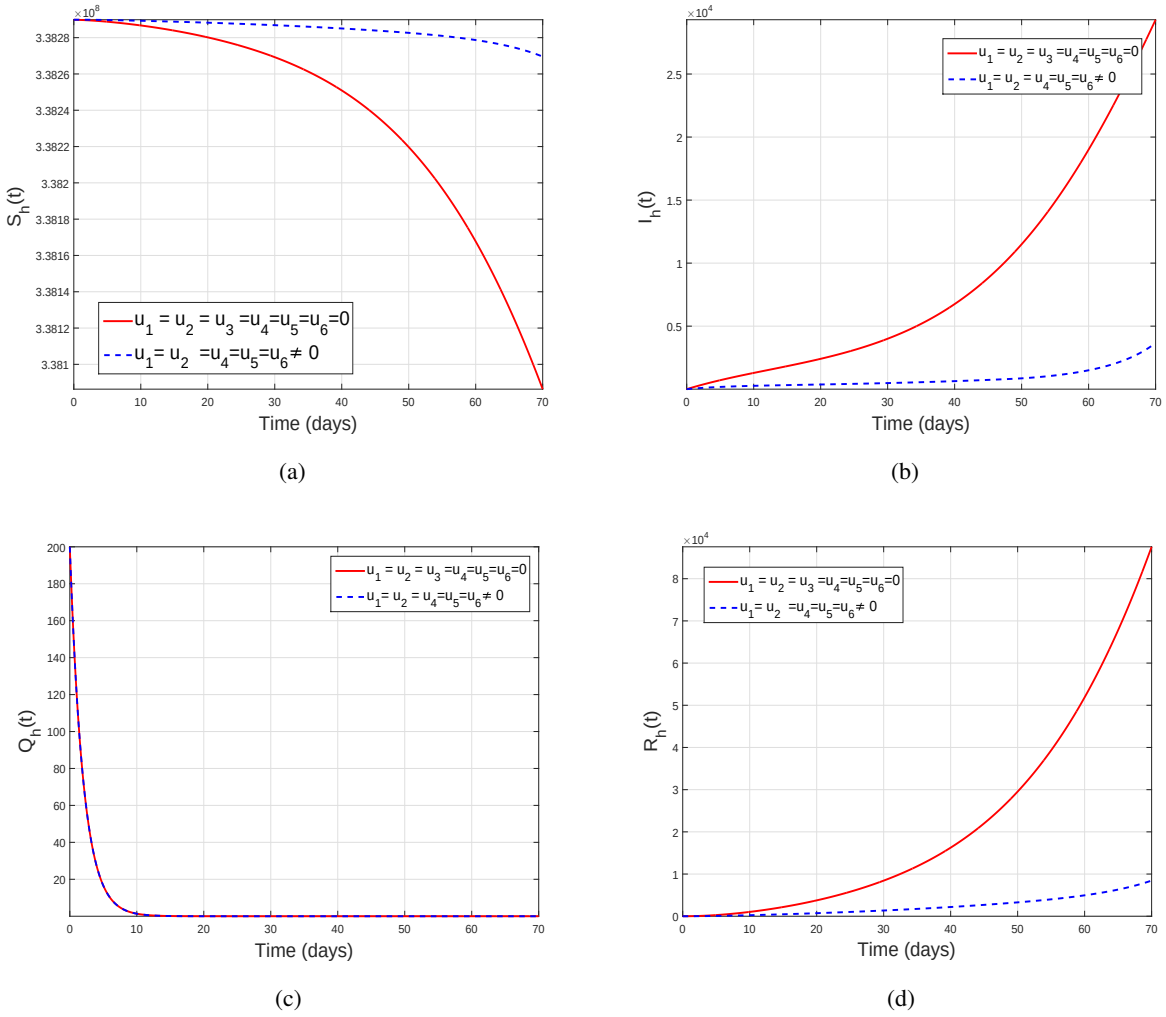

Figure 10. Simulation of the MPX control model (5.1) with considering all control variables except u_3 i.e., $u_1 \neq 0$, $u_2 \neq 0$, $u_4 \neq 0$, $u_5 \neq 0$, $u_6 \neq 0$ and $u_3 = 0$. (a) Susceptible human. (b) Infected human. (c) Isolated human. (d) Recovered human.

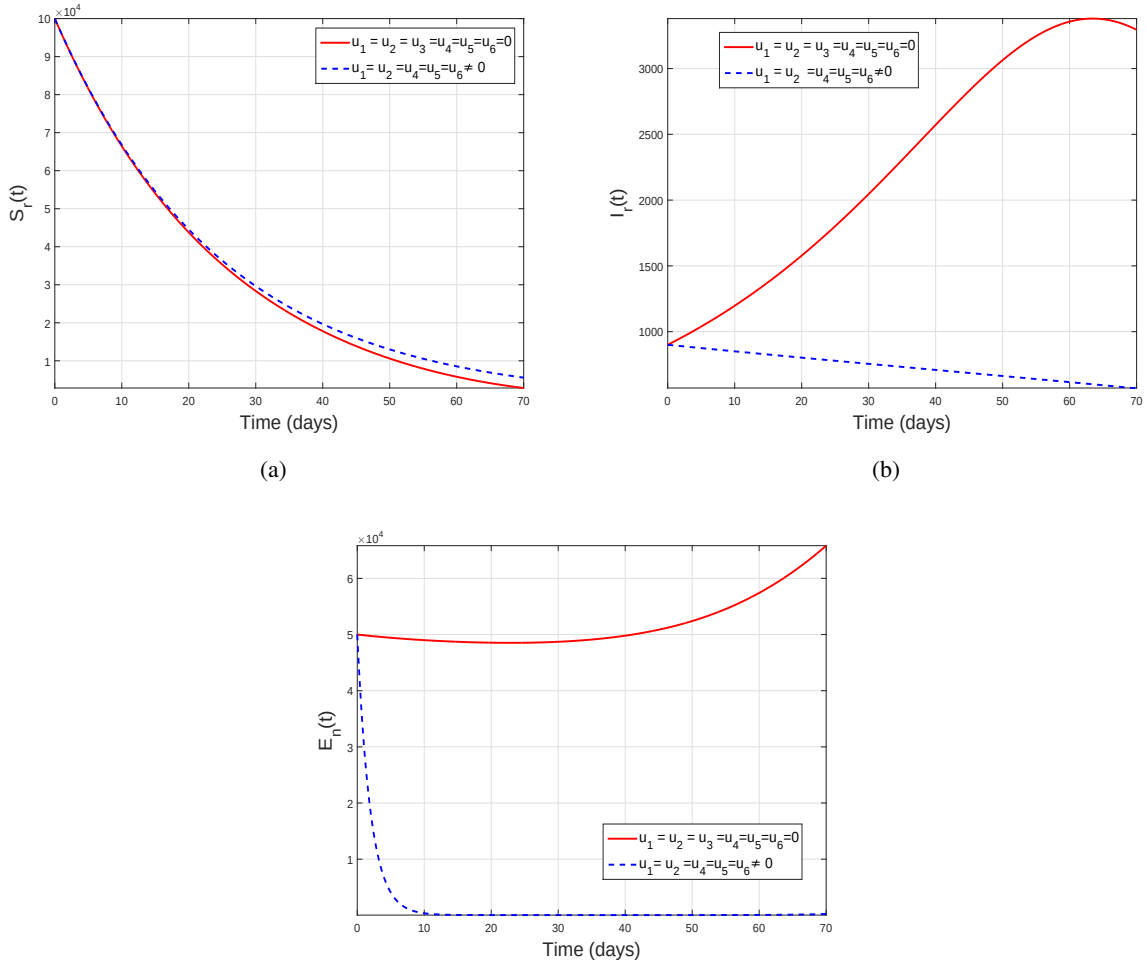

Figure 11. Simulation of the MPX control model (5.1) with considering all control variables except u_3 i.e., $u_1 \neq 0$, $u_2 \neq 0$, $u_4 \neq 0$, $u_5 \neq 0$, $u_6 \neq 0$ and $u_3 = 0$. (a) Susceptible human. (b) Infected human. (c) Environmental viral concentration.

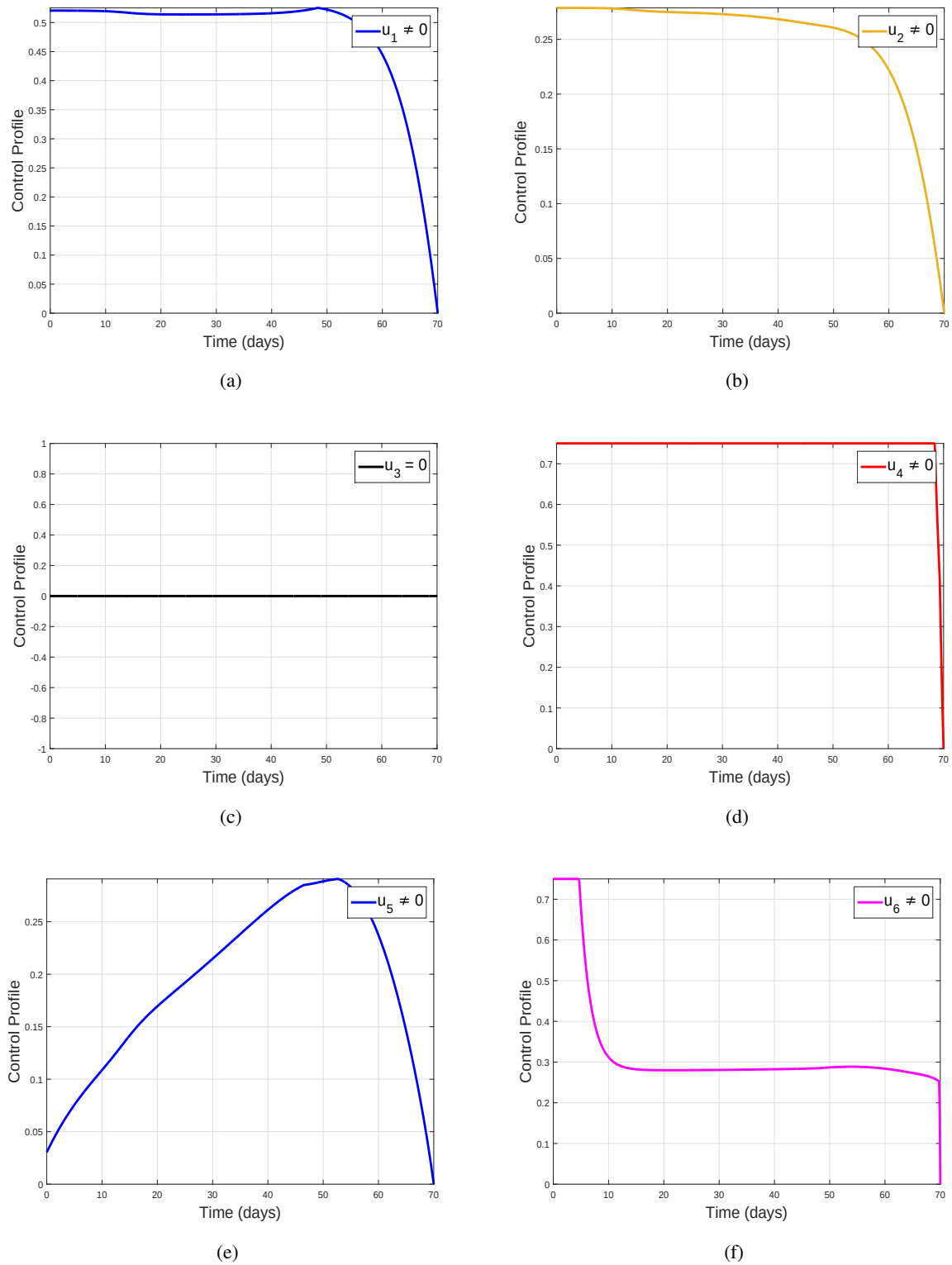

Figure 12. The corresponding control profile for strategy C. (a) u_1, (b) u_2, (c) u_3, (d) u_4, (e) u_5, (f) u_6.

6.4. *Strategy D: using all control variables except u_5 and u_6.*

This strategy presents the impact of personal protection measures and isolation control. The role of this case in infection control is graphically illustrated in Figures 13 and 14. The plots describing control profiles of each optimal control variable in this strategy are depicted in Figure 15. It is observed, that the environmentalviral concentration reduces at a slower rate as compared to previous strategies, as seen in Figure 13(c). Still, it can be used to curtail the infection in a community. Overall, from the simulation of all strategies, we conclude that the best and optimal control intervention that can be used effectively to eradicate the infection is strategy A (i.e., considering all control measures at the same time).

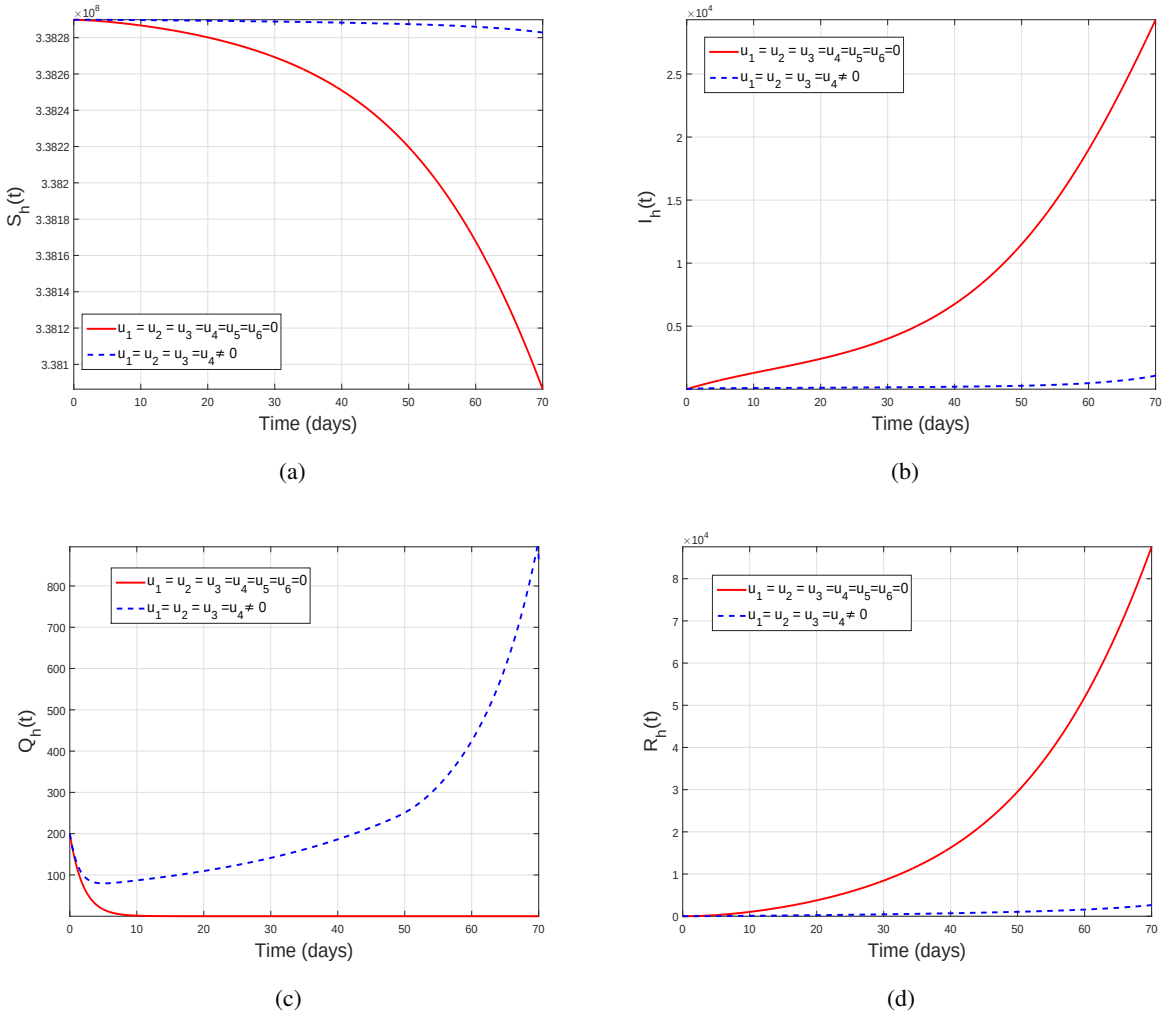

Figure 13. Simulation of the MPX control model (5.1) with considering all control variables except u_5 and u_6. (a) Susceptible human. (b) Infected human. (c) Isolated human. (d) Recovered human.

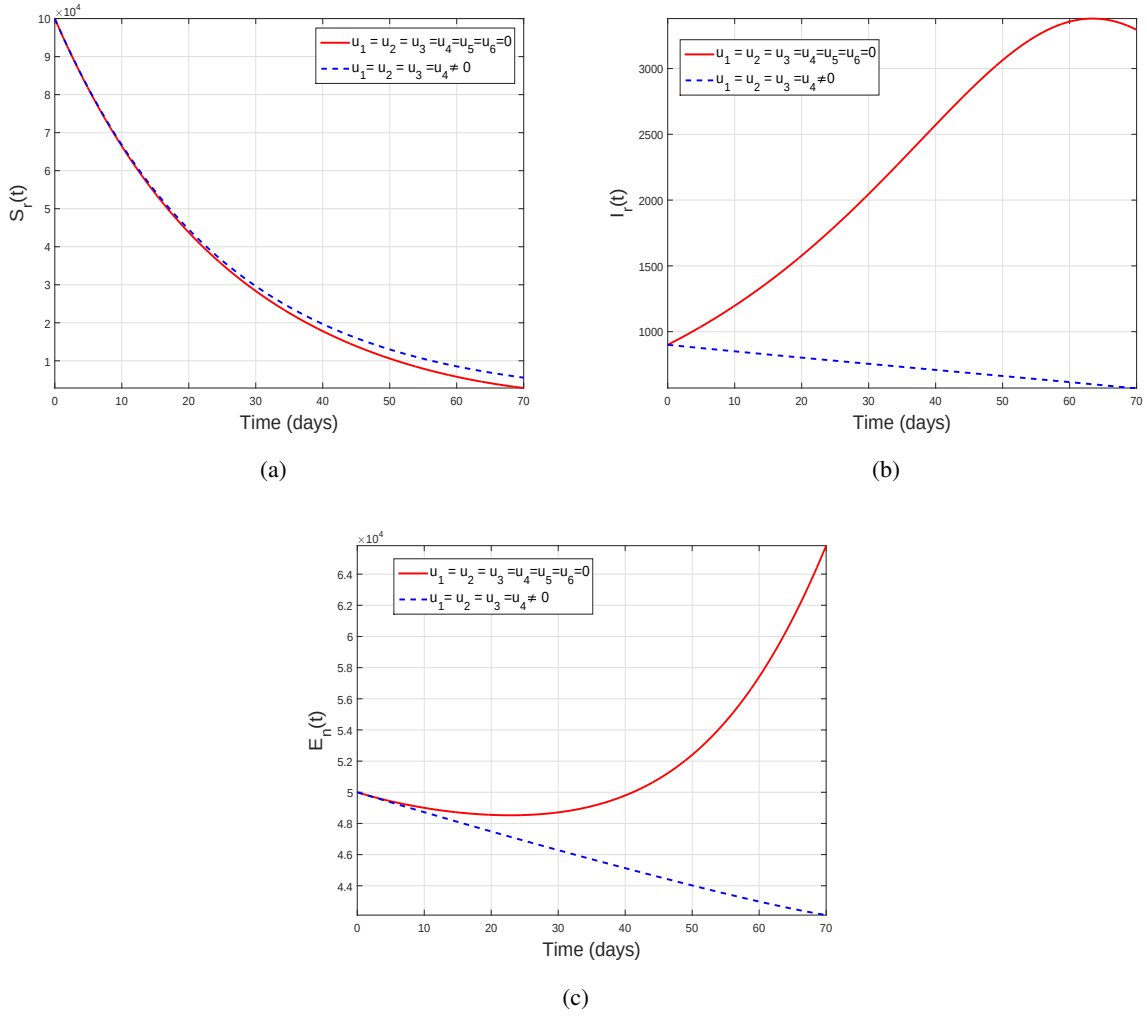

Figure 14. Simulation of the MPX control model (5.1) with considering all control variables except u_5 and u_6. (a) Susceptible human. (b) Infected human. (c) Environmental viral concentration.

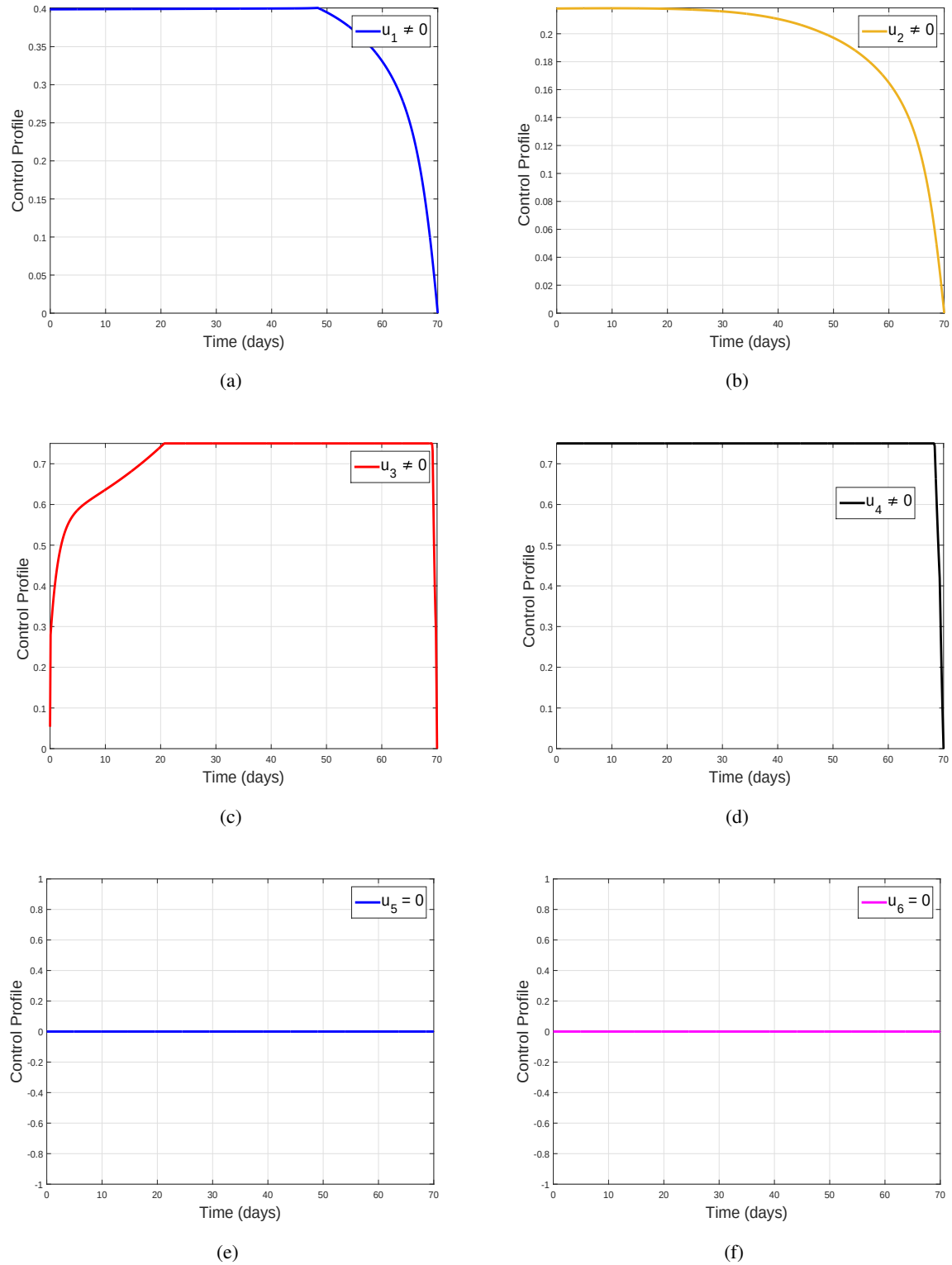

Figure 15. The corresponding control profile for strategy D. (a) u_1 (b) u_2 (c) u_3 (d) u_4, (e) u_5 (f) u_6.

7. Conclusions

Besides the less severity of the MPX infection, it is alarming that a current outbreak is reported in many non-endemic countries. The early eradication of the infection is necessary before it emerges as a new health issue around the globe. In this study, we developed a mathematical model addressing the dynamics of monkeypox under some optimized predictive control interventions. The model parameters are estimated from the reported infected cases during the 2022 outbreak in the USA in order to make the study more useful. The model is first formulated with constant control measures using a nonlinear differential system. The viral concentration in the environment and the environmental transmission are taken into consideration in the model formulation. The model is reformulated by incorporating personal protection measures, isolation control, and fumigating commercial areas. The control interventions are respectively repressed by six time-dependent control variables namely: $u_1(t)$, $u_2(t)$, $u_3(t)$, $u_4(t)$, $u_5(t)$, and $u_6(t)$. The following outcomes of the present study are observed

- The model exhibits a disease-free and endemic equilibria.
- The model is found to be stable locally and globally at the disease-free equilibrium when, $\mathcal{R}_0 < 1$.
- The basic reproduction number is evaluated based on estimated values of model parameters.
- Normalized sensitivity analysis indicates that personal protection measures, isolation control, and fumigating commercial areas are effective to control interventions.
- The usage of time-dependent controls can reduce the total number of infected individuals in the human and animal populations.
- The most effective control intervention involves all control variable simultaneously.

Fractional order modeling are more reliable than the integer epidemic models. Therefore, the present study could be further extended using fractional case modeling with singular and nonsingular kernels.

Acknowledgments

This research work was funded by Institutional Fund Projects under grant no. (IFPIP: 970-130-1443). The authors gratefully acknowledge technical and financial support provided by the Ministry of Education and King Abdulaziz University, DSR, Jeddah, Saudi Arabia.

Conflict of interest

The authors declare no conflicts of interest.

References

1. World Health Organization, *Monkeypox*, 2022. Available from: http:/www.who.int/en/news-room/fact-sheets/detail/monkeypox.
2. D. Bisanzio, R. Reithinger, Projected burden and duration of the 2022 Monkeypox outbreaks in non-endemic countries, *Lancet Microbe*, **3** (2022), e643. https://doi.org/10.1016/S2666-5247(22)00183-5

3. K. N. Durski, A. M. McCollum, Y. Nakazawa, B. W. Petersen, M. G. Reynolds, S. Briand, et al., Emergence of monkeypox–West and central Africa, 1970–2017, *Morbid. Mortal Wkly Rep.*, **67** (2018), 306–310. https://doi.org/10.15585/mmwr.mm6710a5
4. Z. Jezek, M. Szczeniowski, K. M. Paluku, M. Mutombo, B. Grab, Human monkeypox: confusion with chickenpox, *Acta Trop.*, **45** (1988), 297–307.
5. E. Alakunle, U. Moens, G. Nchinda, M. I. Okeke, Monkeypox virus in Nigeria: infection biology, epidemiology, and evolution, *Viruses*, **12** (2020), 1257. https://doi.org/10.3390/v12111257
6. Centers for Disease Control and Prevention, *Monkeypox Vaccination Basics*, 2023. Available from: `https://www.cdc.gov/poxvirus/mpox/vaccines/index.html`.
7. T. Li, Y. Guo, Optimal control and cost-effectiveness analysis of a new COVID-19 model for Omicron strain, *Phys. A: Stat. Mech. Appls.*, **606** (2022), 128134. https://doi.org/10.1016/j.physa.2022.128134
8. P. A. Naik, J. Zu, M. B. Ghori, M. Naik, Modeling the effects of the contaminated environments on COVID-19 transmission in India, *Results Phys.*, **29** (2021), 104774. https://doi.org/10.1016/j.rinp.2021.104774
9. P. A. Naik, J. Zu, K. M. Owolabi, Global dynamics of a fractional order model for the transmission of HIV epidemic with optimal control, *Chaos Solitons Fract.*, **138** (2020), 109826. https://doi.org/10.1016/j.chaos.2020.109826
10. A. Ahmad, M. Farman, P. A. Naik, N. Zafar, A. Akgul, M. U. Saleem, Modeling and numerical investigation of fractional-order bovine babesiosis disease, *Numer. Meth. Part. Differ. Equ.*, **37** (2021), 1946–1964. https://doi.org/10.1002/num.22632
11. S. A. Somma, N. I. Akinwande, U. D. Chado, A mathematical model of monkey pox virus transmission dynamics, *Ife J. Sci.*, **21** (2019), 195–204. https://doi.org/10.4314/ijs.v21i1.17
12. N. O. Lasisi, N. I. Akinwande, F. A. Oguntolu, Development and exploration of a mathematical model for transmission of monkey-pox disease in humans, *Math. Model. Eng.*, **6** (2020), 23–33. https://doi.org/10.21595/mme.2019.21234
13. S. Usman, I. I. Adamu, Modeling the transmission dynamics of the monkeypox virus infection with treatment and vaccination interventions, *J. Appl. Math. Phys.*, **5** (2017), 2335–2353. https://doi.org/10.4236/jamp.2017.512191
14. P. C. Emeka, M. O. Ounorah, F. Y. Eguda, B. G. Babangida, Mathematical model for monkeypox virus transmission dynamics, *Epidemiology*, **8** (2018), 348. https://doi.org/10.4172/2161-1165.1000348
15. O. J. Peter, S. Kumar, N. Kumari, F. A. Oguntolu, K. Oshinubi, R. Musa, Transmission dynamics of Monkeypox virus: a mathematical modelling approach, *Model. Earth Syst. Environ.*, **8** (2022), 3423–3434. https://doi.org/10.1007/s40808-021-01313-2
16. A. M. Alzubaidi, H. A. Othman, S. Ullah, N. Ahmad, M. M. Alam, Analysis of Monkeypox viral infection with human to animal transmission via a fractional and Fractal-fractional operators with power law kernel, *Math. Biosci. Eng.*, **20** (2023), 6666–6690. https://doi.org/10.3934/mbe.2023287

17. C. Madubueze, I. O. O. Onwubuyq, G. N. Nkem, Z. Chazuka, On the transmission dynamics of the monkeypox virus in the presence of environmental transmission, *Front. Appl. Math. Stat.*, **28** (2022), 1–21. https://doi.org/10.3389/fams.2022.1061546

18. Y. Guo, T. Li, Dynamics and optimal control of an online game addiction model with considering family education, *AIMS Math.*, **7** (2022), 3745–3770. https://doi.org/10.3934/math.2022208

19. J. K. Asamoah, Z. Jin, G. Q. Sun, B. Seidu, E. Yankson, A. Abidemi, et al., Sensitivity assessment and optimal economic evaluation of a new COVID-19 compartmental epidemic model with control interventions, *Chaos Solitons Fract.*, **146** (2021), 110885. https://doi.org/10.1016/j.chaos.2021.110885

20. J. K. K. Asamoah, E. Okyere, A. Abidemi, S. E. Moore, G. Q. Sun, Z. Jin, et al., Optimal control and comprehensive cost-effectiveness analysis for COVID-19, *Results Phys.*, **33** (2022), 105177. https://doi.org/10.1016/j.rinp.2022.105177

21. Y. Guo, T. Li, Modeling and dynamic analysis of novel coronavirus pneumonia (COVID-19) in China, *J. Appl. Math. Comput.*, **68** (2022), 2641–2666. https://doi.org/10.1007/s12190-021-01611-z

22. S. Majee, S. Jana, T. K. Kar, Dynamical analysis of monkeypox transmission incorporating optimal vaccination and treatment with cost-effectiveness, *Chaos*, **33** (2023), 043103. https://doi.org/10.1063/5.0139157

23. J. K. Asamoah, Z. Jin, G. Q. Sun, Non-seasonal and seasonal relapse model for Q fever disease with comprehensive cost-effectiveness analysis, *Results Phys.*, **22** (2021), 103889. https://doi.org/10.1016/j.rinp.2021.103889

24. T. Berge, M. Chapwanya, J. S. Lubuma, Y. Terefe, A mathematical model for Ebola epidemic with self-protection measures, *J. Biol. Syst.*, **26** (2018), 107–131. https://doi.org/10.1142/S0218339018500067

25. J. P. Tian, J. Wang, Global stability for cholera epidemic models, *Math. Biosci.*, **232** (2011), 31–41. https://doi.org/10.1016/j.mbs.2011.04.001

26. *United States Population*, 2022. Available from: `https://www.worldometers.info/world-population/us-population/`.

27. P. van den Driessche, J. Watmough, Reproduction numbers and sub-threshold endemic equilibria for compartmental models of disease transmission, *Math. Biosci.*, **180** (2002), 29–48. https://doi.org/10.1016/S0025-5564(02)00108-6

28. A. Hamid, P. Sinha, The impact of media coverage on the dynamics of vector-borne diseases, *Comput. Ecol. Soft.*, **12** (2022), 54–66.

29. C. C. Chavez, S. Blower, P. Driessche, D. Kirschner, A. A. Yakubu, *Mathematical approaches for emerging and reemerging infectious diseases: models, methods, and theory*, Springer Science and Business Media, 2002. https://doi.org/10.1007/978-1-4613-0065-6

30. N. Chitnis, J. M. Hyman, J. M. Cushing, Determining important parameters in the spread of malaria through the sensitivity analysis of a mathematical model, *Bull. Math. Biol.*, **70** (2008), 1272–1296. https://doi.org/10.1007/s11538-008-9299-0

31. W. H. Fleming, R. W. Rishel, *Deterministic and stochastic optimal control*, Springer Science and Business Media, 1975. https://doi.org/10.1007/978-1-4612-6380-7

32. J. K. Hale, *Ordinary differential equations*, Springer New York, 1998. https://doi.org/10.1007/978-1-4612-0601-9

33. L. S. Pontryagin, *Mathematical theory of optimal processes*, CRC press, 1987. https://doi.org/10.1201/9780203749319 .

AIMS Press